



AMERICAN METEOROLOGICAL SOCIETY

Journal of Climate

EARLY ONLINE RELEASE

This is a preliminary PDF of the author-produced manuscript that has been peer-reviewed and accepted for publication. Since it is being posted so soon after acceptance, it has not yet been copyedited, formatted, or processed by AMS Publications. This preliminary version of the manuscript may be downloaded, distributed, and cited, but please be aware that there will be visual differences and possibly some content differences between this version and the final published version.

The DOI for this manuscript is doi: 10.1175/JCLI-D-12-00026.1

The final published version of this manuscript will replace the preliminary version at the above DOI once it is available.

If you would like to cite this EOR in a separate work, please use the following full citation:

Earl, N., S. Dorling, R. Hewston, and R. von Glasow, 2012: 1980-2010 variability in UK surface wind climate. *J. Climate*. doi:10.1175/JCLI-D-12-00026.1, in press.

Abstract

11
12
13 The climate of the north-east Atlantic region comprises substantial decadal variability in
14 storminess. It also exhibits strong inter- and intra-annual variability in extreme high and
15 low windspeed episodes. Here we quantify and discuss causes of the variability seen in
16 the UK wind climate over the recent period 1980-2010. We consider variations in UK
17 hourly windspeeds, in daily maximum gust speeds and in associated wind direction
18 measurements, made at standard 10m height, recorded across a network of 40 stations.
19 The Weibull distribution is shown to generally provide a good fit to the hourly wind data,
20 albeit with shape parameter, k , spatially varying from 1.4-2.1, highlighting that the
21 commonly assumed $k=2$ Rayleigh distribution is not universal. We find that the 10th and
22 50th percentile HM windspeeds have declined significantly over this specific period,
23 whilst still incorporating a peak in the early 1990s. Our analyses place the particularly
24 'low wind' year of 2010 into longer term context and our findings are compared with
25 other recent international studies. Wind variability is also quantified and discussed in
26 terms of variations in the exceedence of key windspeed thresholds of relevance to the
27 insurance and wind energy industries. Associated inter-annual variability in energy
28 density and potential wind power output of the order of $\pm 20\%$ around the mean is
29 revealed. While 40% of network average winds are in the SW quadrant, 51% of energy in
30 the wind is associated with this sector. Our findings are discussed in the context of
31 current existing challenges to improve predictability in the Euro-Atlantic sector over all
32 timescales.

33 1. Introduction

34 Located in one of the most common regions for atmospheric blocking, while also situated
35 towards the end point of a major mid-latitude storm track, the UK has one of the most
36 variable wind climates and NW Europe is a challenging region for prediction on all time
37 scales (Barriopedro et al. 2006 2008; Dacre and Gray 2009; Woollings 2010). Regional
38 wind climate variability in the UK is large, governed by latitude (proximity to storm
39 track), altitude and type of fetch (the UK has an exceptionally long coastline). Seasons
40 dominated by blocking or cyclonic weather types, especially winter, can strongly skew
41 the magnitude of annual insured losses (Munich Re 2002), as well as have profound
42 effects on the variability of wind power generated by the expanding UK wind energy
43 sector (Sinden 2007).

44 The cold European winter of 2009-10 and the extreme cold of December 2010
45 have prompted much discussion about long-term climate variations and their possible
46 impacts. However, Cattiaux et al. (2010) show that the cold European surface
47 temperature anomaly of up to 6°C for winter 2009-10 was in fact not as great as might
48 have been expected given the associated record-breaking North Atlantic Oscillation
49 (NAO) and blocking frequency indices. These authors concluded that the event was a
50 cold extreme which was not in any way inconsistent with an otherwise generally
51 warming climate. Focusing on predictability at the monthly, seasonal and decadal
52 timescale, many forcing agents are thought to modulate European climate, for example
53 sea surface temperatures, stratospheric circulation and solar variability (Rodwell et al.
54 1999; Lockwood et al. 2010 2011; Woollings et al. 2010). Regional responses also arise
55 from the dynamical reaction of the climate system to this forcing (Woollings 2010; Jung

56 et al. 2011) and internal atmospheric dynamics can be an important source of low-
57 frequency atmospheric inter-annual variability. Solar activity in 2009/10 fell to values
58 unknown since the start of the 20th century and Lockwood et al. (2010), linking this to the
59 occurrence of recent cold European winter months, estimate an 8% chance that the
60 decline, which began around 1985, could continue to Maunder minimum levels within 50
61 years, from the previous grand solar maximum. On the other hand ECMWF experiments
62 (Jung et al. 2011), testing the sensitivity to reduced ultra-violet radiation of the onset of
63 the cold 2009-10 European winter, show that the unusually low solar activity contributed
64 little, if any, to the observed NAO anomaly. Much research is ongoing to improve our
65 predictive capability in Europe.

66 In Europe, windstorms remain the most economically significant weather peril
67 when averaging over multiple years. The winter storms of the early 1990s had some
68 dramatic effects on the UK, the winter of 1989-90 being one of the most damaging on
69 record, exemplified by windstorm Daria on 25th January (McCallum 1990). The storm
70 tracked across a large swath of England and Wales, causing widespread damage
71 amounting to £1.9bn (equivalent to £3.2bn in 2010 values) of UK insured losses (Munich
72 Re 2002). A second storm, Vivian, buffeted the UK between 26th and 28th February
73 1990 and contributed to UK weather related property losses that year reaching their
74 highest mark on record. In the winter of 1991-1992 the New Year's Day Storm affected
75 northern Scotland and (far more severely) Norway (Gronas 1995), producing stronger
76 UK surface winds than Daria and Vivian, though causing less UK damage due to reduced
77 vulnerability to insurance losses in the affected regions. Meanwhile winter storm Xynthia
78 in February 2010 caused insured losses totaling almost \$3bn in Germany, France and

79 Spain, representing the world's 3rd most costly catastrophe of that year (Swiss Re 2011),
80 more costly than any 2010 North Atlantic hurricane. Indeed total European windstorm
81 damage is considerable, equivalent to that of worldwide hurricanes when averaged over
82 longer time scales (Malmquist 1999). Total annual losses attributed to windstorms
83 depend, for example, on the precise track and intensities of storms, the relative
84 vulnerability of the affected areas, whether trees are in leaf or not and the relative dryness
85 or wetness of the ground at the time of windstorm passage (Hewston and Dorling 2011).

86 Wang et al. (2009) demonstrated that storminess in the North-Atlantic-European
87 region, based on atmospheric sea-level pressure gradients, undergoes substantial decadal
88 and longer time scale fluctuations and that these changes have a seasonality and
89 regionality to them. In particular, these authors showed that winter storminess reached an
90 unprecedented maximum in the early 1990s in the North Sea and showed a steady
91 increase in the north-eastern part of the North-Atlantic-European region, significantly
92 correlated with variability in the NAO index. The link to the NAO is found in all seasons
93 except autumn. As the NAO swings from one phase to the other, large changes to
94 windstorm intensity and track and to mean windspeed and direction are observed over the
95 Atlantic (Hurrell et al. 2003). Both Atkinson et al. (2006), analyzing the period 1990-
96 2005, and Boccard (2009), 1979–2007, showed that the NAO is a good approximation for
97 synoptic weather type indices such as Grosswetterlagen (Hess and Brezowsky 1952;
98 James 2007) and the Jenkinson-Collinson weather type classification (Jenkinson and
99 Collinson 1977; Jones et al. 1993) and for wind indices in Northern Europe over the
100 respective periods. A decrease in post-1990 northern European windiness is clearly
101 revealed in these studies. By considering the longer term Grosswetterlagen and Jenkinson

102 variability through the 20th century, these authors concluded that care is needed in
103 selecting the most appropriate long-term period on which to base wind energy investment
104 decisions and that access to reliable and longer term windspeed measurements is highly
105 desirable. Recent industry discussion of the low-wind year of 2010 requires further
106 supporting analysis and discussion of the wider context. As greater reliance on wind
107 power for the UK's electricity generation needs increases, so will the magnitude of risk
108 due to exposure of the performance of the turbines to climate change (Harrison et al.
109 2008).

110 Both the wind energy and insurance industries are sensitive to windspeed
111 distributions. The Weibull distribution function has become widely used in meteorology
112 to estimate how observed windspeeds tend to vary around their mean at sites where only
113 a long term average is known. Originally used to describe the size distribution of
114 particles, the Weibull distribution has numerous applications, including in general
115 insurance to model reinsurance claim sizes (Kremer 1998). The use and importance of the
116 Weibull distribution has grown immensely in the wind power industry and has been used
117 to help site many thousands of wind turbines (Petersen et al. 1998; see section 2c).

118 Numerous authors have also been considering the possible impact of climate
119 change over the 21st century on the wind climate of north-west Europe, in the context of
120 the decadal variability seen over the last century (Brown et al. 2009; Ulbrich et al. 2009;
121 Pryor et al. 2011). While this is clearly a complex question, one point which models do
122 seem to currently agree on for the future climate of the region is an increasing frequency
123 of intense cyclones in the region of the British Isles (Ulbrich et al. 2009) and increased
124 winter storminess (Scaife et al. 2011).

125 Hewston (2006) and Hewston and Dorling (2011) introduced for the first time an
126 hourly windspeed database for a network of 43 UK surface stations, extending through
127 the period 1980-2005 and providing good spatial coverage. Based on this they presented
128 a climatology of the strongest wind gusts in the context of insurance weather perils.
129 These authors presented evidence of an apparent downward trend in the strongest wind
130 gusts over the UK since the early 1990s. In addition, Vautard et al. (2010), also using
131 surface station data, reported that mean windspeeds have also been declining over the
132 same period across most areas of the world, including Europe, a phenomenon which they
133 termed “global stilling” and which they linked to changes in land-based biomass.
134 However, while a decline was also found in Australian 2m windspeed observations by
135 Troccoli et al. (2012), their equivalent 10m measurements actually showed a positive
136 tendency.

137 Here we build on the earlier UK-focused work of Hewston and Dorling (2011)
138 described above by also considering mean windspeeds in the UK. The objectives of this
139 paper are to

- 140 • Update analysis of temporal variability to 2010 and extend the quality control of
141 the Hewston and Dorling database.
- 142 • Deepen understanding of each of the stations in the network by investigating
143 applicability of the Weibull distribution across locations, interpreting the results
144 from a topographic perspective.
- 145 • Analyze variations of exceedences of a wider range of windspeed thresholds of
146 interest to both the insurance and wind energy sectors, compare these with the

147 larger-scale findings of Vautard et al. (2010) and discuss them in the context of
148 key features of the regional-scale atmospheric circulation.

- 149 • Quantify the impact of the observed spatial and temporal variations in wind power
150 on output from a synthetic network of 3.6MW wind turbines, one located at each
151 of the monitoring stations.

152

153 The results presented in this paper include analysis and discussion of windspeed
154 threshold exceedence frequencies, the proportion of time that the hourly winds or daily
155 gust speeds are above a set of specific speeds, at individual sites and on average across
156 the network of 40 (39) hourly windspeed (gust speed) sites. This follows the approach
157 adopted by Vautard et al. (2010) but provides detail for the UK rather than a more
158 general continental or global scale. The further novelty of the study presented here comes
159 from using hourly data, rather than 6-hourly, by considering a high spatial density of
160 stations in the UK, by incorporating gusts and wind directions with mean windspeeds and
161 by including the anomalous conditions of 2010. Furthermore we present the implications
162 of a variable wind climate for wind energy density and wind power output, building on
163 the work of previous UK wind resource studies (e.g. Sinden 2007).

164

165 2. Data, methods and tools

166 a. *Observed Wind Data*

167 This study extends the 1980-2005 database described by Hewston and Dorling
168 (2011) of hourly surface windspeed observations (measured at the standard 10m height)

169 from UK Meteorological Office (UKMO) stations across the UK, to the end of 2010,
170 incorporating the anomalous European winter months in 2010. Wind data for all 31 years
171 were extracted from the MIDAS (Met Office Integrated Data Archive System) Land
172 Surface Observations Station database (UKMO 2011), archived at the British
173 Atmospheric Data Centre (BADC). Unfortunately, three of the 43 sites used in the
174 original network (Coltishall, Durham and St Mawgan) have been discontinued since 2005
175 and have been removed from the database. The hourly mean (10-minute average,
176 recorded from 20 to 10 minutes prior to the hour in question; hereafter HM) windspeeds
177 and daily maximum gust speeds (DMGS; maximum 3 second average), with their
178 associated wind directions, are extracted as described in detail by Hewston and Dorling
179 (2011). The site at Ringway (Manchester Airport) no longer records gusts, only mean
180 windspeeds, leaving a 31 year (1980–2010) UK network of 40 sites for HM windspeeds
181 and 39 sites for DMGSs whose geographical locations are displayed in Fig.1. Hewston
182 and Dorling's (2011) primary focus was the DMGSs, whereas this study makes more use
183 of the HM windspeeds. The 40 sites used in this study have on average 98.5% HM data
184 completeness, substantially higher than previous studies using HM MIDAS data (e.g
185 Sinden 2007, 77% HM data completeness). All of the sites used in this study meet the
186 stringent UKMO site exposure requirements (available at
187 http://badc.nerc.ac.uk/data/ukmo-midas/ukmo_guide.html). Since the sites in this study
188 possess such a wide variety of topographies and therefore wind regimes, it is thought that
189 when averaged together they give a good representation of the UK wind regime as a
190 whole.

191 *b. Data quality*

192 The windspeed and direction data has undergone rigorous quality control, with checks on
 193 the equipment and raw data performed at the UKMO and the BADC. Further information
 194 on quality control performed on the MIDAS database and other possible sources of error
 195 is available at the BADC website ([http://badc.nerc.ac.uk/data/ukmo-](http://badc.nerc.ac.uk/data/ukmo-midas/ukmo_guide.html)
 196 [midas/ukmo_guide.html](http://badc.nerc.ac.uk/data/ukmo-midas/ukmo_guide.html)) (UKMO 2011) and in Hewston and Dorling (2011). Once
 197 downloaded, a series of steps were followed to further test the reliability of the
 198 information, removing duplicate data, detecting missing values and checking data
 199 consistency. Analysis of Weibull distributions, discussed below, was also helpful in
 200 highlighting potential anomalies. The MIDAS data does not normally include an HM
 201 value of 1 knot (0.515 ms^{-1}) and often uses a value of 2 knots (1.03 ms^{-1}), when the wind
 202 vane indicates gusty conditions (BADC website), to represent a mean speed of 0 or 1
 203 knot. This leads to an over-representation of HM wind values of 2 knots and an under-
 204 representation of 0 and especially 1 knot at many sites. We have, however, made no
 205 attempt to re-distribute these extra 2kt values into neighboring bins.

206 *c. Weibull distribution*

207 The Weibull distribution came to prominence in meteorology during the 1970s
 208 (Takle and Brown 1977). As a two-parameter density function it can be calculated as

$$209 \quad P(U) = 1 - \exp\left[-\left(\frac{U}{A}\right)^k\right] \quad (1)$$

210 Where $P(U)$ is the probability distribution of windspeed U , A is the Weibull scale
 211 parameter and k is the shape parameter (Pryor and Barthelmie 2010). For a narrow
 212 distribution, with a marked peak, k will take a relatively high value. Numerous statistical

213 methods have been proposed to calculate Weibull scale and shape parameters (Pryor et al.
214 2004), Seguro and Lambert (2000) recommending the maximum likelihood method when
215 windspeed data is available in a time series format. When the Weibull shape parameter
216 has a value of 2, it is known as the Rayleigh distribution, and this is often used as the
217 standard for wind turbine manufacturers' performance figures (Weisser 2003). The
218 Weibull distribution, however, has been found to produce a better fit to observed
219 windspeeds than the simpler Rayleigh distribution (Celic 2004).

220 Nevertheless it is problematic fitting a Weibull distribution at low windspeeds, as
221 highlighted by Justus et al. (1976) who assessed potential output from wind-powered
222 generators. On the other hand, it is generally accepted that sites with regular moderate or
223 high windspeeds can almost always be approximated by the Weibull distribution
224 (Petersen et al.1998), Jamil et al. (1995) estimating this moderate windspeed threshold to
225 be 12 ms^{-1} or higher. It would therefore be expected that a Weibull distribution would
226 more realistically simulate a DMGS distribution than an HM distribution.

227 Both the 31 year UK HM windspeed and DMGS data can be used to assess
228 whether the Weibull distribution function is a good fit to these observations. The HM
229 data contains periods of low windspeeds (including many calm hours/periods) which
230 have been highlighted as not being well represented by the Weibull distribution. The
231 DMGS set however, by definition, should be more Weibull compatible. This study
232 examines the capability of the Weibull distribution to represent the variance of land-
233 based wind monitoring sites, by calculating the 31-year shape parameter at each site for
234 both HM windspeed and DMGSs. This also reveals how well the commonly used
235 Rayleigh distribution approximates the sites' windspeed variance. There have been

236 numerous methods and modifications to the Weibull distribution to deal with zero and
237 low windspeed values, however it is not the intention here to assess which of these best
238 represents the DMGS and HM datasets, therefore this study simply uses the commonly
239 adopted basic maximum likelihood method (Seguro and Lambert 2000). It must be noted
240 that the basic method used is unable to accommodate calm conditions, although the
241 approach can be modified to account for these (Wilks 1990). Tests were carried out
242 assigning a negligible value (0.00001 ms^{-1}) to reports of 0 ms^{-1} , however the results for
243 HM windspeeds (not shown) displayed strong positively skewed, poorly fitting Weibull
244 distributions and k values as low as 0.3.

245 *d. Wind turbine power*

246 The 31 year UK HM windspeed database enables an assessment of the potential impact
247 of spatial and temporal variations in the UK wind regime on the wind energy sector.
248 Power generated is proportional to the cube of the windspeed and the variability of the
249 wind around the mean is therefore critical to the amount of power produced. Wind power
250 generation potential can be quantified using the concept of energy density (aka power
251 density)

252
$$E = \frac{1}{2} \rho U^3 \quad (2)$$

253

254 where E is energy density (W m^{-2}), ρ is air density (kg m^{-3}) and U is the hub-height
255 windspeed (ms^{-1}) (Pryor 2011). For this study, the energy density for each of the 40 HM
256 observation sites is calculated to first-order with equation (2), using an air density of
257 1.225 kg m^{-3} (15°C at sea level) and assuming negligible density variations (Pryor et al.
258 2004; Jamil et al. 1995), ignoring altitude and temperature variability between sites

259 (which could theoretically lead up to an associated $\pm 8\%$ air density variation compared to
 260 the average value adopted).

261 A limitation of the applicability of the energy density quantity is that even the
 262 most modern wind turbines cannot harvest power below and above specific windspeed
 263 thresholds (Table 1). Outside this range, the windspeed is either too low to turn the blades
 264 or too high, forcing the turbine to be shut down in order to prevent damage (AEA 2011).
 265 Based purely on the cubic relationship between windspeed and power generation, energy
 266 density returns an overestimation of wind turbine performance, especially during stormy
 267 periods such as the early 1990s. For comparison, another method is also used to quantify
 268 wind turbine performance to second-order, including cut-in and cut-out windspeed
 269 thresholds and sensitivity to windspeed variations within that range (Oswald et al. 2008).
 270 For each of the 40 HM observation sites, a synthetic state of the art 3.6MW wind turbine
 271 is considered for the duration of the recorded observations and the 10m winds are
 272 adjusted to the typical hub height of 100m using the power law approximation, ignoring
 273 the important effect of variable atmospheric stability and surface roughness (z_0) for this
 274 simple estimate (Petersen et al. 1998; Motta et al. 2005).

$$275 \quad \frac{U(z_1)}{U(z_2)} = \left(\frac{z_1}{z_2} \right)^p \quad (3)$$

276

277 Where $U(z_1)$ and $U(z_2)$ are the windspeeds at heights z_1 and z_2 , respectively, and p is the
 278 power law exponent taken to be equal to 0.14 (Petersen et al. 1998) (giving $U_{100} = U_{10} \times$
 279 1.38). The value of p typically ranges from 0.05 (very unstable atmosphere with
 280 $z_0=0.01\text{m}$) to 0.69 (stable atmosphere with $z_0=3\text{m}$), the adopted value 0.14 representing a
 281 neutral atmosphere for a small z_0 (0.01-0.1m) and a typical value for areas with variable

282 stability (Irwin 1979). Once the height conversion has been performed, the power output
283 is then estimated for each hour at each site based on the power output curve of the
284 3.6MW wind turbine (Table 1). Energy density and power output are calculated for each
285 site and averaged across the network, weighting for any missing data, and the observed
286 temporal variability is discussed.

287 *e. North Atlantic Oscillation*

288 The HM and DMGS 1980-2010 windspeed database presents an excellent opportunity to
289 investigate the relationship between the NAO index and UK windspeeds and assess the
290 impacts of the phase changes of the NAO on land based wind measurements and wind
291 energy output estimates. This furthers the work of Cheng et al. (2011) who used satellite
292 observations to investigate inter-annual variability of high wind occurrence in the North
293 Atlantic over the period 1988-2009. The particular NAO index used for this study is
294 based on normalized sea-level pressure observations made at Gibraltar and Reykjavik in
295 Iceland, with homogeneous records that date back to the 1820s, allowing for a long term
296 monthly NAO index (Jones et al. 1997) [available on the University of East Anglia's
297 Climatic Research Unit (CRU) website:
298 <http://www.cru.uea.ac.uk/~timo/datapages/naoi.htm>; hereafter CRU website]. There are
299 numerous methods to calculate the NAO index, however this monthly index has the
300 advantage of the longest record, helping place the 1980-2010 UK HM wind variability
301 into context (see <http://www.cru.uea.ac.uk/cru/info/nao/> for more detail).

302 3. Results and discussion

303 *a. Inter-annual variability*

304 Fig. 2 shows a timeseries of annual average 10m HM windspeeds in the form of the 10th,
305 50th and 90th percentiles, quantifying the inter-site variability. The 10th and 50th percentile
306 5-year moving averages exhibit peaks in the early 1980s and early 1990s, with a general
307 statistically significant decrease visible over the full 1980-2010 period (confidence levels
308 of 99.9% and 95% for the 10th and 50th percentiles respectively; using ordinary least
309 squared linear regression analysis). The 90th percentile shows a much more pronounced
310 early 1990s peak, without the general decline seen in the 10th and 50th percentiles, but
311 with a statistically significant decrease since 1990 (at the 99% level). The 10th and 50th
312 percentiles show that in the mid-late 2000s windspeeds began to recover, however the
313 anomalously low winds of 2010, discussed in detail below, are at odds with this recovery.
314 Fig. 2 highlights large year to year variability in windspeeds for all percentiles, for
315 example the median varying from 4.3-5.3 ms⁻¹. Our results and those of other authors
316 highlight the presence of strong decadal variability and we include linear trend analyses
317 here only for completeness. Behind these results from the network as a whole, it should
318 be noted that 32 of the 40 sites display a decrease in annual mean windspeed over the full
319 period, 15 of which are statistically significant (95% confidence level), while 8 show an
320 increase, 2 of which are statistically significant. There is no clear geographical pattern to
321 the distribution of stations exhibiting statistically significant changes.

322 To learn more about the nature of winds experienced in the UK over the 1980-
323 2010 period, several HM windspeed exceedence thresholds were selected and the
324 frequency of exceedence at each site calculated. Fig. 3 displays results, expressed as a

325 network average, for two particular thresholds, 11ms^{-1} and 13ms^{-1} , a ‘strong breeze’ on
326 the Beaufort scale. These thresholds have been chosen here because when adjusted to
327 wind turbine hub height, 3.6MW wind turbines begin to work at full capacity (Table 1).
328 Furthermore, all of the 40 sites in the network experience such windspeeds, unlike for
329 higher thresholds which are only exceeded at a minority of sites. Throughout the paper,
330 we have chosen to focus on wind speed thresholds which are both consistent with those
331 highlighted by Vautard et al (2010) and, especially, on those for which it is known that
332 building damage of varying degrees would be expected. It is acknowledged however that
333 the latter actually vary with geography according to build quality as show by Klawe and
334 Ulbrich (2003) and so the implication of our threshold results should be seen as indicative
335 only.

336 The proportion of time when the network average HM windspeed exceeds the
337 11ms^{-1} threshold ranges from just over 2% of the time in 2010, due to the cold and
338 relatively calm months of January and December that year (see 2010 windspeed and
339 direction in Fig. 4d), to 6.7% in 1990, associated with the storminess of January and
340 February. The inter-annual variation is striking with, for an extreme example, 1986
341 experiencing winds in excess of 11ms^{-1} for twice as many hours as in the previous and
342 following years, a feature also reported by Vautard et al. (2010) for Europe as a whole,
343 though less pronounced. The 13ms^{-1} threshold exceedences exhibit a similar pattern to
344 that of 11ms^{-1} ranging between just below 1% and just below 3% also in 2010 and 1990,
345 respectively. The early 1980s and early 1990s, particularly the latter, have the highest
346 proportion of HM windspeeds over each threshold, with a statistically significant
347 decrease from 1980 (95% and 99% confidence for 13ms^{-1} and 11ms^{-1} exceedences

348 respectively). The more intense threshold exceedence peak in the early 1990s compared
349 with that of the early 1980s is in keeping with the 90th percentile of the HM annual
350 average windspeed shown in Fig. 2. This reinforces the findings of Wang et al. (2009),
351 suggesting a more volatile wind regime in the early 1990s with more 10m winds reaching
352 in excess of 11ms^{-1} and 13ms^{-1} but with a lower average windspeed compared to the early
353 1980s.

354 Figs. 2 and 3 reveal a large change between the adjacent years 1986 and 1987,
355 1986 recording far higher windspeeds. To further investigate this difference, network
356 average wind roses were produced for both years (Fig. 4b and c; along with the 1980-
357 2010 climatology (a) and the extreme year of 2010 (d)), 1986 revealing a much more
358 pronounced tendency for south-westerly winds. This is to be expected with stronger
359 south-westerly winds associated with the extra-tropical cyclone storm track. Increased
360 south-westerly winds are positively correlated with the NAO (Cheng et al. 2011) and the
361 monthly NAO index is significantly more positive in January, October, November and
362 December in 1986 than in the equivalent 1987 months.

363 The peaks of the early 1980s and early 1990s are further highlighted by the five
364 year running mean of network average HM windspeed threshold exceedence shown in
365 Fig. 5, though the early 1980's peak is not as pronounced as in the 10th and 50th
366 percentiles of site HM windspeeds shown in Fig. 2. In Fig. 5, in addition to the 11ms^{-1}
367 and 13ms^{-1} exceedence thresholds shown in Fig. 3, further thresholds of 3ms^{-1} , 5ms^{-1} ,
368 7ms^{-1} , 9ms^{-1} and 15ms^{-1} are also included. Although the logarithmic scale somewhat
369 reduces the visual impact of the variability, nevertheless a statistically significant
370 decrease ($\geq 99\%$ confidence) over the last 20 years remains visible for exceedence

371 thresholds in the range $7\text{-}15\text{ms}^{-1}$. As expected, the contribution of individual sites to the
372 total exceedence percentage varies throughout the network, especially as the exceedence
373 thresholds rise and become of interest for the insurance sector. This is discussed in detail
374 below (section 3e), with Fig. 10a highlighting the site contribution variations for the
375 15ms^{-1} threshold.

376 One of the findings of Vautard et al. (2010) was a general decline in European
377 windspeeds over the last 30 years, especially for extreme winds, whereas UK results
378 presented here more strongly emphasize an early 1990s peak and a marked decline over
379 the last 20 years, highlighting the importance of not assuming a simple overall linear
380 trend. We might not be surprised by this difference due to the UK's location on the edge
381 of Europe, more exposed to the Atlantic, compared to the continental scale of the Vautard
382 et al. (2010) study. Results presented here extend and are consistent with the UK, NAO
383 and Grosswetterlagen indices presented by Atkinson et al. (2006) and with the broader
384 spatial scale findings of Wang et al. (2009) and Boccard (2009).

385 The DMGS exhibits a similar long-term variability to that of the HM as depicted
386 by the five year moving average of network average DMGS threshold exceedence shown
387 in Fig. 6. Higher thresholds are included here compared with the HM analysis, ranging
388 from 9ms^{-1} - 35ms^{-1} , revealing peaks in the early 1980s and early 1990s with the
389 exception of the highest 35ms^{-1} exceedence threshold which does not have such a marked
390 peak in the early 1980s but a more extreme maximum in the running mean around
391 1991/2. The 35ms^{-1} 1980-2010 decline is statistically significant (with 99% confidence)
392 accommodating a peak in 1993, with the windspeed exceeding the threshold 0.5% of
393 days (at all sites), compared to 2001 and 2010 when this threshold was not breached at all

394 (not shown). Lerwick (station 40) and Kirkwall (39), in the Northern Isles (Fig. 1),
395 contributed to 16 and 15 days respectively of the total 69 DMGS values in excess of this
396 extreme wind threshold in 1993 (not shown). Note that 20ms^{-1} is generally accepted as a
397 starting DMGS threshold for minor structural damage in connection with insurance
398 claims.

399 Sensitivity tests of the inter-annual variability of threshold exceedences to the
400 network configuration have been carried out (not shown), based on the removal of the
401 most significant contributor stations to the 15 (HM) and 25ms^{-1} (DMGS) exceedence
402 thresholds in Figs. 5 and 6 respectively. While the removal of these stations leads to
403 inevitable quantitative changes of exceedence percentage, the interpretation of the
404 periods of enhanced and reduced exceedence remains unchanged, indicating low
405 sensitivity to specific station choice.

406 *b. North Atlantic Oscillation – driver of temporal wind climate variations*

407 Positive peaks in the NAO index are seen in the early 1980s and particularly in
408 the early 1990s when the 10-year Gaussian-weighted filter was at its highest during the
409 whole 189 year time period (CRU website). The decrease since the early 1990s is
410 apparent, and partly explains the declining tendency in HM and DMGS UK wind
411 observations and DMGSs over the last 20 years as shown in Figs. 2, 3, 5 and 6. The
412 winter of 2009/10 had substantially more negative NAO index than any other winter
413 measured during the record (Osborn 2011), explaining the anomalously low windspeeds
414 observed. The consecutive winters 1994/5 and 1995/6 produced the greatest year to year
415 contrast since the NAO series began in 1823, however this was not seen in the station
416 observations (Figs. 2, 3, 5 and 6) showing that winter NAO index is not the only

417 important factor contributing to the UK wind regime and hence the importance of
418 studying intra-annual variability as discussed below.

419 To investigate the effects that the NAO index variations have on the observed UK
420 wind climate, two network average wind roses are presented in Fig. 7, highlighting the
421 difference in windspeed and direction observed during months when the NAO index is in
422 strong negative (≤ -2) and strong positive phase (≥ 2). When the NAO is in strong
423 positive phase, observed winds are stronger and very much dominated by the south-west
424 sector, whereas during periods of strong negative phase, the speeds are more often lower
425 and the direction much more evenly spread, with a greater tendency for north-easterlies.
426 During negative NAO phase, the anomalous increase in pressure over Iceland suppresses
427 westerly winds, diverting the storm track southwards over the Mediterranean and
428 encouraging a more northerly and easterly flow over the UK (Hurrell et al. 2003).

429 *c. Intra-annual variability*

430 The considerable intra-annual wind variation in the UK is highlighted in Fig. 8 by the
431 seasonal network averages of HM windspeed for 15ms^{-1} threshold exceedences. The
432 winter peak of HM windspeeds exceeding 15ms^{-1} during the early 1990s is apparent,
433 displaying the impact of the associated intense winter storminess (Wang et al. 2009). The
434 statistically significant winter decline since 1990 (99% confidence) is particularly
435 marked, generally following a similar progression to that of the NAO winter time series.
436 The winter of 1989/90 witnessed the highest 15ms^{-1} threshold exceedence percentage of
437 $\sim 3.5\%$, with the lowest (complete) winter being in 2009/10, exceeding 15ms^{-1} just 0.3%
438 of the time, lower than in most autumn and spring seasons.

439 The spring 15ms^{-1} exceedence percentage (Fig. 8) generally hovers around 0.5%,
440 peaking at over 1% in 1994. Autumn meanwhile does not reveal a peak during the early
441 1990s, but was more extreme instead at the start of the observation period during the
442 early 1980s and also peaked in the late 1990s before declining once more, partially
443 consistent with the findings of Vautard et al. (2010), during 1979 - 2008, that the most
444 substantial linear decrease in Europe occurred in the autumn season in this particular
445 period. The relatively high 15ms^{-1} exceedences of the early 1980s in autumn is consistent
446 with the early 1980s peak in UK observations (Figs. 2, 3, 5 and 6) are not as apparent in
447 the NAO winter time series. Meanwhile, summer season threshold exceedences remain
448 low and relatively consistent throughout the observation period. From this we can deduce
449 that the threshold exceedence peak of the early 1980s is associated with higher winds in
450 both winter and autumn seasons, whereas the early 1990s peak is caused mainly by the
451 winter storminess alone.

452 As the seasonal variation of the HM wind exceedence threshold of 15ms^{-1} is so
453 strong, especially between winter and summer, we show in Fig. 9 the network average
454 wind direction distribution for each season over the 1980-2010 period. All of the seasons
455 are dominated, on average, by winds from the south-west quadrant, winter unsurprisingly
456 having the strongest such winds, associated with the storm track moving south during the
457 northern hemisphere winter (Dacre and Gray 2009). Autumn has a similar looking wind
458 rose to that of winter, whereas summer and spring have different appearances, summer
459 having a more influential north-west quadrant (and lower windspeeds overall) and spring
460 a more significant north-easterly component. During summer the Atlantic westerlies are
461 less dominant with the storm track pushed north by the Azores High, leading to

462 climatologically more high pressure systems centred to the west of the UK producing
463 comparatively more north-westerly winds. This means that summer winds are generally
464 less extreme in speed despite the increase in thunderstorm activity seen in the summer
465 and the associated potential for damaging downdrafts (Wheeler and Mayes 1997).
466 Conditions during spring and early summer are more favorable for blocking situations
467 over northern Europe (Barriopedro et al. 2006), leading to comparatively more wind with
468 a north-easterly component as confirmed in Fig. 9b.

469 *d. Spatial variability*

470 When dealing with the network average of exceedence thresholds, spatial
471 variability is hidden. Spread across the UK, the network sites possess characteristics that
472 vary considerably, both in topography and exposure to the storm track (Fig. 1). Exposure
473 to fetch over the Atlantic Ocean and Irish Sea is important, along with the latitude and
474 altitude; the higher and further north a site is, the stronger the wind due to reduced
475 friction and greater proximity to the higher storm track density region to the south and
476 east of Iceland (Dacre and Gray 2009). Surface roughness and vegetation also play key
477 roles as highlighted by Vautard et al. (2010). These points in mind, the relative
478 contributions of each site to threshold exceedence, especially for higher thresholds, are
479 expected to vary significantly. Fig. 10 shows the relative contributions of each site to the
480 exceedences of HM 15ms^{-1} (speed at which insured property damage begins) and 25ms^{-1}
481 windspeed thresholds over the period 1980-2010, the circle size representing the
482 contribution percentage. The 15ms^{-1} site contributions are dominated by the west coast
483 sites exposed to the Atlantic and Irish Sea, for example Aberporth (station 13 – Fig. 1)
484 and Ronaldsway (27), while the two sites furthest north, Kirkwall (39) and Lerwick (40),

485 also make up more than 25% of the exceedences. This is unsurprising considering that
486 the latter areas, closer to the Icelandic low, are susceptible to more intense storms,
487 especially during positive NAO (Serreze et al. 1997). Meanwhile the west coast stations
488 experience reduced friction when flow is onshore. This is further highlighted in the 25ms^{-1}
489 site contribution map (Fig. 10b) with even more weight towards exposed sites and the
490 most northerly Kirkwall (39) and Lerwick (40) stations.

491 Inland sites rarely contribute to either exceedence threshold compared with their
492 more coastal neighbors. The inland northern sites of Eskdalemuir (31) and Salsburgh (33)
493 are situated only 50 miles from each other and have similar altitudes of 242 and 277m
494 respectively, however Salsburgh contributes far more to the 15ms^{-1} and 25ms^{-1}
495 exceedence thresholds (just under 10% for each), with Eskdalemuir not exceeding 25ms^{-1}
496 at all during the 1980-2010 period. Eskdalemuir is situated in a north-south orientated
497 valley, with tree covered ridges on either side, whereas the Salsburgh monitoring site is
498 located on an exposed grass covered hill with a large flat top to the north and east.
499 Centrally located in Scotland's heavily populated central belt, Salsburgh is broadly
500 representative of the insurance risks associated with windstorms transitioning across this
501 important area. The Salsburgh- Eskdalemuir contrast is highlighted in the 1980-2010 HM
502 wind roses in Fig. 10, with wind direction distribution affected by the site characteristics,
503 meaning that Eskdalemuir is somewhat sheltered from the strong westerly winds. Many
504 of the site characteristics are highlighted by their respective wind roses, with Bala (17)
505 located in a south-west to north-east orientated valley in Snowdonia, dominated by south-
506 westerly and north-easterly winds, whereas the relatively flat and open site of Heathrow
507 possesses a similar wind direction distribution to that of the network average with a

508 prevailing south-westerly (Fig. 4a). Table 2 shows the network average proportion of
509 wind direction for each quadrant of the compass, revealing that despite the south-westerly
510 predominance, there is an easterly component to the UK HM wind 38.1% of the time.

511 Wind roses are shown for the directions of HM winds exceeding the thresholds of
512 15ms^{-1} and 25ms^{-1} , to confirm where the strongest winds originate (Fig. 11). The 15ms^{-1}
513 and the 25ms^{-1} thresholds are dominated by south-westerly winds with the south-west
514 quadrant ($190^\circ - 270^\circ$) accounting for 59.9 and 78.9% respectively, as Hewston and
515 Dorling (2011) found for extreme (top 2%) DMGSs.

516 The DMGS 1980-2010 39-site network average wind rose (not shown) is similar
517 to that of the HM (Fig. 4a), with the proportion of wind direction for each quadrant
518 (Table 2) also extremely similar. This is the same when comparing individual site HM
519 wind roses (Fig. 10) with equivalent DMGS wind roses (not shown). This suggests that
520 the factors, be it site aspect, local scale flow or synoptic scale flow which contribute to
521 the direction of HM winds, are the same for DMGSs.

522 *e. Application of the Weibull function to describe windspeed distributions*

523 The spatial variation of windspeeds in the UK is considerable, as shown above, and this
524 contrast is also seen when the Weibull distribution is fitted to the HM and DMGS data.
525 Fig. 12 shows the relationship between the Weibull shape parameter (k) and mean
526 windspeed at each of the 40 HM locations, along with histograms for some prominent
527 sites. Generally there is a slight positive correlation (not statistically significant) between
528 mean windspeed and k . The spread of k ranges from ~ 1.45 – 2.1 , values similar to those
529 reported in the literature by Celik (2004) based on hourly observations in Turkey (1.1-
530 1.89), and by Pryor et al. (2004) for buoy measurements around the coast of North

531 America (1.4-2.5). Different Weibull parameter calculation methods and ways of dealing
532 with zero values have an effect (see section 2c), along with the fact that the locations
533 used in this study are geographically heterogeneous leading to highly varied wind
534 regimes. Just 6 out of the 40 sites have k values of more than the commonly used
535 Rayleigh distribution value of 2 and the majority of sites range from 1.7 - 1.9
536 highlighting the dangers of simply using the Rayleigh distribution to describe wind
537 distributions for wind farm siting.

538 The Weibull distribution describes the observed HM winds well as shown by the
539 histograms in Fig. 12. The Weibull distribution provides a better fit to the sites with
540 comparatively few low windspeeds, as shown when comparing the sites of Lerwick (40)
541 and Kirkwall (39) to Eskdalemuir (31) and East Malling (8). This is partly due to the
542 method of low value recording in the MIDAS database producing an overrepresentation
543 of 2 knots (1.03ms^{-1}) at certain sites (e.g. Eskdalemuir (31) and Heathrow (10)). This
544 slightly negatively skews the Weibull distribution and affects the k values. It is also due
545 to the nature of the Weibull distribution best approximating well measured sites with
546 moderate or high windspeeds (Petersen et al. 1998).

547 Weibull shape parameter (k) values seem to be a function of both the strength of
548 the mean wind and the impact of site characteristics. Sites with very low windspeeds such
549 as East Malling (8) produce low values of k, due to the high counts of low wind values,
550 however other sites with higher means but with anomalous wind roses (varying greatly
551 from that of the network average, affected by local site characteristics – Fig. 10) such as
552 Bala (17) and West Freugh (30) also have low k (not shown), associated with topographic
553 effects such as local valley flows. Sites with low means but evenly distributed (similar to

554 network average) wind roses like Heathrow (10) (Fig. 10) and Nottingham (18) (not
555 shown) have relatively high k with regard to mean wind (Fig. 12). Valley (22) has high
556 mean windspeed but is located in a valley, so local topography affects the wind direction
557 and windspeed distributions.

558 The Weibull distribution does not approximate the DMGS distribution as
559 accurately as for the HM winds as shown by Fig. 13. The k values are much higher than
560 for the HMs, ranging between ~ 2.4 and ~ 2.9 , which is unsurprising given that the use of
561 the DMGS metric eliminates many low values. The windspeed threshold of 12 ms^{-1}
562 required for good Weibull fit according to Jamil et al. (1995) seems not to be reliable for
563 DMGSs, with sites possessing averages above and below 12 ms^{-1} , being underestimated
564 for the most frequent values and overestimated for the lower windspeeds (Fig. 13).
565 Generally the tails of the distributions are well approximated for the higher average
566 DMGS sites and slightly overestimated for the sites with lower average DMGS.

567 *f. Wind energy implications*

568 The HM windspeeds have been converted into network average energy density and
569 potential power output (PPO) of a synthetic wind turbine network. Table 2 highlights just
570 how important the SW quadrant is for wind power production. Both methods show
571 significant year to year variability of power output over the 1980-2010 period (Fig. 14),
572 as originally seen in the annual average percentile HM windspeeds (Fig. 2), in the HM
573 threshold exceedences (Figs. 3, 5), in the DMGS threshold exceedences (Fig. 6) and in the
574 NAO index (CRU website). Peaks in energy density and PPO are seen in the early 1980s
575 and early 1990s and are clearly displayed by the 5 year moving averages. The anomalous
576 year of 2010 stands out in both energy metrics, representing the lowest values of the

577 whole period; the extreme variability of consecutive years 1986-7 is also clear. The main
578 difference between the two methods is the more marked peak in the early 1990s in energy
579 density. The unprecedented storminess described by Wang et al. (2009) of the early
580 1990s produced the most extreme winds of the period in the UK, often above the cut-out
581 speed of even the most modern and largest turbines. The 10m windspeeds of above 18ms⁻¹
582 are too high to be captured by the 3.6 MW turbines in the PPO, but account for
583 extremely high levels of energy production in the energy density output (Table 1) due to
584 the cubic relationship with windspeed. The PPO results are in accordance with those of
585 Sinden (2007) during corresponding years of study. In addition the load factor of 30% is
586 in keeping with the predetermined value used in the Sinden (2007) study. This load factor
587 was found by Sinden to approximate the UK wind power output figures well, especially
588 since 1997.

589 The range of annual mean PPO is large, 867-1265kW (2010 and 1986
590 respectively) with an average of 1087 kW. During the highest production year, the
591 synthetic 3.6MW wind turbine network was working on average at 35% efficiency (aka
592 load factor; with the assumption of steady winds) and at 24% efficiency for the lowest
593 production year. The year 1986 saw 16 % more energy generated than the 1980-2010
594 average whereas 2010 was 20% below. The energy produced in 1987 was just 73% of
595 that of 1986, a much larger difference than the inter-annual variability in wind energy
596 density that Petersen et al. (1998) found across many regions in Europe ($\pm 10 - 15\%$). This
597 shows that basing wind farm decisions on a single year of monitored data can be a
598 dangerous practice (Brayshaw et al. 2011).

599 The demand for electricity in the UK fluctuates strongly, varying from hourly to
600 annual timescales (Pöyry 2011). Users need electricity at different times of the year for
601 different reasons (eg summer cooling demand and warming in winter) (Sinden 2007),
602 which may not match the periods of low and high wind output (AEA 2011). Winter is the
603 season when electrical power output is most important, with colder temperatures and
604 shorter days, domestic and commercial users require energy for heating and lighting, so
605 how does our synthetic wind turbine network simulate seasonal PPO variation over the
606 1980-2010 period? Fig. 15 shows the evolution of seasonal mean PPO, highlighting the
607 prominence of the winter season, though not as dominant in power production as might
608 be expected given the dominance of winter windiness (Fig. 8). The efficiency of synthetic
609 power harnessed is at its greatest in winter 1995 (47% efficiency), and at its lowest (18%)
610 in summer 1983. PPO is very low in the winter of 2009-10 and comparable to the
611 summer averages. This shows that storage and backup generation schemes will become
612 crucial to energy suppliers in the future, with ever increasing reliance on wind power and
613 other renewable sources.

614 4. Conclusions and outlook

615 The characteristics of the UK HM and DMGS wind regimes, with applications to the
616 insurance and wind energy industries, are presented here, based on data from a 40-station
617 wind monitoring network over the continuous 1980-2010 period. The main findings are
618 summarized as follows:

619

- 620 • The 10th and 50th (but not the 90th) percentile HM windspeeds have declined
621 significantly over this specific period, whilst still incorporating a peak in the early
622 1990s. 2010 recorded the lowest annual 10th and 90th percentile and second lowest
623 (behind 1987) 50th percentile windspeed over the whole 1980-2010 period [Fig.
624 2]. This is all, however, in the context of longer term decadal variability.
- 625
- 626 • The Weibull distribution is more suited to representing HM winds rather than
627 DMGS distributions at typical land-based sites, the former revealing site-specific
628 shape parameter values ranging from 1.4-2.1 [Fig. 12] somewhat in contrast with
629 the often assumed k=2 Rayleigh distribution, with associated implications for
630 turbine site selection.
- 631
- 632 • As the HM exceedence thresholds rise, the early 1980s peak in exceedence
633 frequency diminishes, while the early 1990s peak becomes more apparent [Fig.
634 5], with a declining tendency since, confirming the early 1990s unprecedented
635 peak in NE Atlantic winter storminess reported by Wang et al. (2009). This is not
636 fully consistent with Vautard et al. (2010) who highlighted a temporally broader
637 decline for the whole of Europe over the period 1979-2008.
- 638
- 639 • The DMGS exceedence thresholds exhibit similar variations to those of the HM,
640 with the highest thresholds (30 and 35 ms⁻¹) displaying the most marked early
641 1990s peak and a decline since [Fig. 6], indicating that the decrease of extreme

642 DMGSs highlighted by Hewston and Dorling (2011) has continued through to
643 2010, contributing to the reduction in UK storm-related insurance claims.

644

645 • The network average 1980-2010 HM prevailing wind direction is in the south-
646 west quadrant (40% of the time). However significant seasonal and inter-annual
647 variation is apparent in the relative frequency of all wind directions and this needs
648 to be accounted for in wind energy assessments.

649

650 • The 40% frequency in south-west quadrant winds translates into a 51% proportion
651 of energy in the wind [Table 2].

652

653 • The range of network average annual mean Potential Power Output is significant,
654 from -20% to +16% around the average, with the synthetic energy produced in
655 1987 just 73% of the previous year, 1986, and 2010 the lowest producing year of
656 all [Fig. 14].

657

658 The recent variability in UK mean wind and gust climate, including the particularly
659 anomalous atmospheric circulation patterns of 2010, quantified and discussed here,
660 naturally leads to related questions about the future, both within the scientific community
661 and from other stakeholders. 2010 was an anomalously low wind year, a relatively bad
662 year for wind energy production but a good year for the insurance industry in terms of
663 reduced claims volumes. The two sectors are, however, also positively related if one

664 considers the growing underwriting role that insurance is now playing, reducing the risk
665 of weather-sensitive wind energy revenue streams.

666 Future climate projections have a large spread between models and low signal-to-
667 noise ratio over Europe compared with other mid-latitude areas (Hawkins & Sutton
668 2009), Europe being one of the hardest regions for which to predict weather and climate
669 on all timescales (Woollings 2010; Ulbrich et al. 2009). Recent extreme events such as
670 the European winter of 2009-10 have led to alternative causal interpretations, including
671 an emphasis on the important role of recent declining solar output (Lockwood et al. 2010,
672 2011) and on internal dynamical responses to varied forcing (Jung et al. 2011). While
673 further research seeks to improve models and reduce key uncertainties, both in the
674 prediction of extreme event onset and of persistence, it seems wise to anticipate further
675 significant variability in the UK wind climate and concentrate upon building resilience to
676 this.

677 *Acknowledgements*

678 This research was kindly funded by the Worshipful Company of Insurers, and was
679 carried out at the University of East Anglia. Thanks must go to the BADC and UK Met
680 Office for providing the windspeed data. Interested parties wishing to access the observed
681 windspeed data may, for research purposes, apply for access through the BADC. Thanks
682 must also go to Ben Webber and Jennifer Graham at the University of East Anglia for
683 help with data processing and the development of figures.

684

685

686 **References**

- 687 AEA, 2011: Evaluation of the climate risks for meeting the UK's carbon budgets. *Report*
688 *for Committee on Climate Change ED56732- 3*. [Available online at
689 http://hmccc.s3.amazonaws.com/Progress%202011/ED56732_FinalReport_FINALv2.pdf]
690
- 691 Atkinson, N., K. Harman, M. Lynn, A. Schwarz, and A. Tindal, 2006: Long-term
692 Windspeed Trends in Northwestern Europe. Garrad Hassan [Available online at
693 <http://w.bwea.com/pdf/28proceedings/Tindal%20paper.pdf>]
- 694 Barriopedro, D., R. Garcia-Herrera, and R. Huth, 2008: Solar modulation of Northern
695 Hemisphere winter blocking. *J. Geophys. Res.* **113**, D14118.
696 doi:10.1029/2008JD009789
- 697 Barriopedro, D., R. Garcia-Herrera, A. R. Lupo, and E. Hernández, 2006: A climatology
698 of Northern Hemisphere Blocking. *J. Climate.* **19**, 1042-1063.
- 699 Boccard, N., 2009: Capacity factor of wind power realized values vs. estimates. *Energ.*
700 *Policy.* **37**, 2679-2688.
- 701 Brayshaw, D .J., A. Troccoli, R. Fordham, and J. Methven, 2011: The impact of large
702 scale atmospheric circulation patterns on wind power generation and its potential
703 predictability: A case study over the UK. *Renew Energ.* **36**, 2087-2096.
- 704 Brown, S., P. Boorman, R. McDonald, and J. Murphy, 2009: Interpretation for use of
705 surface windspeed projections from the 11-member Met Office Regional Climate
706 Model ensemble. UKCP09 Tech. Note. 22 pp.

- 707 Cattiaux, J., R. Vautard, C. Cassou, P. Yiou, V. Masson-Delmotte, and F. Codron, 2010:
708 Winter 2010 in Europe: A cold extreme in a warming climate. *Geophys. Res. Lett.*
709 **37**, L20704. doi:10.1029/2010GL044613
- 710 Celik, A. N., 2004: A statistical analysis of wind power density based on the Weibull and
711 Rayleigh models at the southern region of Turkey. *Renew Energ*, **29** 593–604.
- 712 Cheng, X., S. Xie, H. Tokinaga, and Y. Du, 2011: Interannual variability of high-wind
713 occurrence over the North Atlantic. *J. Climate*. doi: 10.1175/2011JCLI4147.1.
- 714 Dacre, H. F., and S. L. Gray, 2009: The Spatial Distribution and Evolution
715 Characteristics of North Atlantic Cyclones. *Mon. Weather. Rev.* **137**, 99-115.
- 716 Gronas, S., 1995: The seclusion intensification of the New Year's day storm 1992. *Tellus*
717 **47A**, 733–746.
- 718 Harrison, G., L. C. Cradden, and J. P. Chick, 2008: Preliminary assessment of climate
719 change impacts on the UK onshore wind energy resource. *Energ. Source.* **30 (14)**,
720 1286-1299.
- 721 Hawkins, E., and R. Sutton, 2009: The potential to narrow uncertainty in regional climate
722 predictions. *Bull. Am. Meteor. Soc.* **90**, 1095-1107.
723 doi:10.1075/2009BAMS2607.1
- 724 Hess, P., and H. Brezowsky, 1952: Katalog der Grosswetterlagen Europas. Ber Dt
725 Wetterdienstes in der US-Zone, Nr 33; 39 pp.
- 726 Hewston, R., 2006: Weather, Climate and the Insurance Sector. PhD Thesis. University
727 of East Anglia.
- 728 Hewston, R., and S. R. Dorling, 2011: An analysis of observed maximum wind gusts in
729 the UK. *J. Wind. Eng. Ind. Aerod.* **99**, 845-856. doi:10.1016/j.jweia.2011.06.004

- 730 Hurrell, J. W., Y. Kushnir, G. Ottersen, and M. Visbeck, 2003: *The North Atlantic*
731 *Oscillation: Climate Significance and Environmental Impact*. Amer. Geophys.
732 Union. 279 pp.
- 733 Irwin, J. S., 1979: A theoretical variation of the wind profile power-law exponent as a
734 function of surface roughness and stability. *Atmos. Environ.* **13**, 191–194.
- 735 James, P. M., 2007: An objective classification method for Hess and Brezowsky
736 Grosswetterlagen over Europe. *Theor. Appl. Climatol.* **88(1)**, 17-42.
- 737 Jamil, M., S. Parsa, and M. Majidi, 1995: Wind power statistics and evaluation of wind
738 energy density. *Renew. Energ.* **6(5)**, 623–8.
- 739 Jenkinson, A. F., and F. P. Collison, 1977: An initial climatology of gales over the North
740 Sea. Tech. report. *Synoptic Climatology Branch Memorandum No. 62*,
741 Meteorological Office
- 742 Jones, P. D., M. Hulme, and K. R. Briffa, 1993: A comparison of Lamb circulation types
743 with an objective classification scheme. *Int. J. Climatol.* **13**, 655-663.
- 744 Jones, P. D., T. Jonsson, and D. Wheeler, 1997: Extension to the North Atlantic
745 Oscillation using early instrumental pressure observations from Gibraltar and
746 South-West Iceland. *Int. J. Climatol.* **17**, 1433-1450.
- 747 Jung, T., F. Vitart, L. Ferranti, and J. Morcrette, 2011: Origin and predictability of the
748 extreme negative and NAO winter of 2009/10. *Geophys. Res. Lett.* **38**, L07701.
749 doi:10.1029/2011GL046786.
- 750 Justus, C. G., W. R. Hargraves, and A. Yalcin, 1976: Nationwide assessment of potential
751 output from wind powered generators. *J. Appl. Meteorol.* **15**, 673-678.

- 752 Klawa, M., U. Ulbrich, 2003: A model for the estimation of storm losses and the
753 identification of severewinter storms in Germany. *Nat. Hazards Earth Syst. Sci.* 3,
754 725-732.
- 755 Kremer, E., 1998: Largest claims reinsurance premiums for the Weibull model. *Blätter*
756 *der deutschen Gesellschaft für Versicherungsmathematik.* 279–284.
- 757 Lockwood, M., R. G. Harrison, T. Woolings, and S. K. Solanki, 2010: Are cold winters
758 in Europe associated with low solar activity? *Environ. Res. Lett.* **5(2)**.
759 doi:10.1088/1748-9326/5/2/024001
- 760 Lockwood, M., R. G. Harrison, M. J. Owens, L. Barnard, T. Woollings, and F.
761 Steinhilber, 2011: The solar influence on the probability of relatively cold UK
762 winters in the future. *Environ. Res. Lett.* **6(3)**. doi:10.1088/1748-9326/6/3/034004
- 763 Malmquist, D. L., Ed., 1999: European windstorms and the North Atlantic Oscillation:
764 Impacts, characteristics, and predictability. Vol. 1. Bermuda Biological Station for
765 Research, Risk Prediction Initiative, No. 2, 21 pp
- 766 McCallum, E., 1990: The Burns' day storm, 25 January 1990. *Weather* **45**, 166–173.
- 767 Motta, M., R. J. Barthelmie, and P. Vølund, 2005: The influence of nonlogarithmic wind
768 speed profiles on potential power output at Danish offshore sites. *Wind Energ.* **8**,
769 219–236.
- 770 Munich Re, 2002: Winter Storms in Europe (II) - Analysis of 1999 Losses and Loss
771 Potentials. Munich Reinsurance Company, Munich
- 772 Osborn, T. J., 2011: Winter 2009/2010 temperatures and a record-breaking North
773 Atlantic Oscillation index. *Weather.* **66**, 19-21.
- 774 Oswald, J., M. Raine, A. Ashraf-Ball, 2008: Will British weather provide reliable

- 775 electricity? *Energ. Policy*. **36**, 3212–3225.
- 776 Petersen, E. L., N. J. Mortensen, L. Landberg, J. Hojstrup, and P. F. Helmut, 1998: Wind
777 power meteorology, Part I: climate and turbulence. *Wind Energy*. **1**, 25–45.
- 778 Pryor, S. C., M. Nielsen, R. J. Barthelmie, and J. Mann, 2004: Can satellite sampling of
779 offshore windspeeds realistically represent windspeed distributions? Part II:
780 quantifying uncertainties associated with sampling strategy and distribution fitting
781 methods. *J. Appl. Meteorol.* **43**, 739–750.
- 782 Pryor, S. C., and R. J. Barthelmie, 2010: Climate change impacts on wind energy: a
783 review. *Renew Sust. Energ. Rev.* **14**, 430–437.
- 784 Pryor, S. C., R. J. Barthelmie, N. E. Clausen, M. Drew, I. MacKellar, and E. Kjellström,
785 2011: Analyses of possible changes in intense and extreme windspeeds over
786 northern Europe under climate change scenarios. *Clim Dynam.*
787 doi:10.1007/s00382-010-0955-3
- 788 Rodwell, M. J., D. P. Rowell, and C. K. Folland, 1999: Oceanic forcing of the wintertime
789 North Atlantic Oscillation and European climate. *Nature*, **398**, 320–323.
- 790 Scaife, A. A., T. Spanghehl, D. Fereday, U. Cubasch, U. Langematz, H. Akiyoshi, S.
791 Bekki, P. Braesicke, N. Butchart, M. Chipperfield, A. Gettelman, S. Hardiman,
792 M. Michou, E. Rozanov, and T. G. Shepherd, 2011: Climate Change Projections
793 and Stratosphere-Troposphere Interaction, *Clim Dynam.* In Press
794 doi:10.1007/s00382-011-1080-7
- 795 Seguro, J. V., and T. W. Lambert, 2000: Modern estimation of the parameters of the
796 Weibull windspeed distribution for wind energy analysis. *J. Wind. Eng. Ind.*
797 *Aerod* **85(1)**, 75–84.

- 798 Serreze, M. C., F. Carse, R. G. Barry, and J. C. Rogers 1997: Icelandic Low Cyclone
799 Activity: Climatological Features, Linkages with the NAO, and Relationships
800 with Recent Changes in the Northern Hemisphere Circulation. *J. Climate*. **10**,
801 453-464.
- 802 Sinden, G., 2007: Characteristics of the UK wind resource: Long-term patterns and
803 relationship to electricity demand. *Energ. Policy*. **35**, 112-127
- 804 Swiss Re, 2011: Natural Catastrophes and man-made disasters in 2010: a year of
805 devastating and costly events. Sigma 40
- 806 Takle, E. S., and J. M. Brown, 1978: Note on the use of Weibull statistics to characterize
807 wind-speed data. *J. Appl. Meteorol.* **17(4)**, 556–559.
- 808 Troccoli, A., K. Muller, P. Coppin, R. Davy, C. Russel, and A. L. Hirsch, 2011: Long-
809 term wind speed trends over Australia. *J. Climate*. **25**, 170-183.
810 doi:10.1175/2011JCLI4198.1
- 811 UKMO, 2011: Met Office Surface Data Users Guide. [Available online at
812 http://badc.nerc.ac.uk/data/ukmomidas/ukmo_guide.html#5.5].
- 813 Ulbrich, U., G. C. Leckebusch, and J. G. Pinto, 2009: Extra-tropical cyclones in the
814 present and future climate: a review. *Theor. Appl. Climatol.* **96**, 117-131.
- 815 Vautard, R., J. Cattiaux, P. Yiou, J. Thépaut, and P. Ciais, 2010: Northern Hemisphere
816 atmospheric stilling partly attributed to an increase in surface roughness. *Nat.*
817 *Geosci.* **3**, 756-761. doi: 10.1038/NGE0979
- 818 Wang, X. I., F. W. Zwiers, V. R. Swail, and Y Feng, 2009: Trends and variability of
819 storminess in the Northeast Atlantic region, 1874-2007. *Clim. Dynam.* **33**, 1179-
820 1195.

- 821 Weisser, D., 2003: A wind energy analysis of Grenada: an estimation using the ‘Weibull’
822 density function. *Renew. Energ.* **28**, 1803–12.
- 823 Wilks, D. S. 1990: Maximum likelihood estimation for the gamma distribution using data
824 containing zeros. *J. Climate.* **3**, 1495–1501.
- 825 Wheeler, D., J. Mayes 1997: *Regional Climates of the British Isles*. London, Routledge,
826 437 pp
- 827 Woollings, T., M. Lockwood, G. Masato, C. Bell, and L. Gray, 2010: Enhanced signature
828 of solar variability in Eurasian winter climate. *Geophys. Res. Lett.* **37**, L20805.
829 doi:10.1029/2010GL044601
- 830 Woollings, T., 2010: Dynamical influences on European climate; an uncertain future.
831 *Phil. T. R. Soc. A.* **368**, 3733–3756. doi:10.1098/rsta.2010.0040
- 832
- 833
- 834
- 835
- 836
- 837
- 838
- 839
- 840

841 **List of Figures**

842 FIG. 1. Location of observation stations in the network. Note that Ringway (23) has no
843 DMGS data, only recording hourly mean windspeed.

844 FIG. 2. 10th, 50th and 90th percentiles of annual average HM windspeeds (ms^{-1}), 1980-
845 2010, from the 40- station network.

846 FIG. 3. Network average threshold exceedence percentages for 11 and 13ms^{-1} HM
847 windspeeds.

848 FIG. 4. Network average HM wind roses for 1980-2010 (a), 1986 (b), 1987 (c) and 2010
849 (d).

850 FIG. 5. Network average 5-year running mean HM threshold exceedence percentages for
851 3, 5, 7, 9, 11, 13 and 15ms^{-1} HM windspeeds.

852 FIG. 6. Network average 5-year running mean threshold exceedence percentages for 9,
853 11, 13, 15, 20, 25, 30 and 35ms^{-1} DMGS.

854 FIG. 7. 1980-2010 network average HM wind roses when NAO index is ≥ 2 (a) and ≤ -2
855 (b).

856 FIG. 8. Network average threshold exceedence percentages for 15ms^{-1} HM windspeeds
857 during each season, winter (DJF), spring (MAM), summer (JJA) and autumn (SON) (note
858 that the winter of 1980 only includes Jan and Feb 1980 and the winter of 2010 only
859 includes Dec 2010).

860 FIG. 9. Network average HM seasonal wind roses, 1980-2010, winter (a), spring (b),
861 summer (c) and autumn (d).

862 FIG. 10. Contribution (percentage) of each site to 15 ms^{-1} (a) (total counts 74154) and 25
863 ms^{-1} (b) (total counts 323) HM windspeed threshold exceedence plus selected all-
864 windspeed 1980-2010 individual site wind roses.

865 FIG. 11. 1980-2010 HM wind roses for exceedences of 15ms^{-1} (a - total counts 74154)
866 and 25ms^{-1} (b - total counts 323) thresholds (all sites).

867 FIG. 12. HM windspeeds compared with Weibull shape parameter, k , for each site plus
868 selected site wind distributions.

869 FIG. 13. DMGSs compared with Weibull shape parameter for each site, along with
870 selected site DMGS distributions.

871 FIG. 14. Bottom – Network average energy density (W m^{-2}). Top - network average
872 potential power output (kW) of a synthetic network of 100m hub height 3.6MW wind
873 turbines.

874 FIG. 15. Network average seasonal mean potential power output (kW) of a synthetic
875 network of 100m hub height 3.6MW wind turbines (note that the winter of 1980 only
876 includes Jan and Feb 1980 and the winter of 2010 only includes Dec 2010).

877

878 TABLE 1. Power produced by a present-day state of the art 3.6MW wind turbine and
 879 Energy Density (from equation 2) for windspeeds in the range 0-26 m s⁻¹ converted to
 880 100m using the power law approximation (equation 3).

Surface windspeed m s ⁻¹	Windspeed m s ⁻¹ at 100m	Power kW	Energy Density W m ⁻²
0	0	0	0
1	1.38	0	1.61
2	2.76	0	12.88
3	4.14	102	43.46
4	5.52	361	103.02
5	6.90	770	201.21
6	8.28	1386	347.69
7	9.67	2175	553.84
8	11.04	2965	824.16
9	12.42	3411	1173.47
10	13.80	3565	1609.69
11	15.18	3595	2142.50
12	16.56	3600	2781.55
13	17.95	3600	3542.42
14	19.33	3600	4423.86
15	20.71	3600	5440.59
16	22.09	3600	6602.27
17	23.47	3600	7918.54
18	24.85	3600	9399.08
19	26.23	0	11050.50
20	27.61	0	12888.75
21	28.99	0	14920.34
22	30.37	0	17154.93
23	31.75	0	19602.18
24	33.13	0	22271.77
25	34.51	0	25173.35
26	35.89	0	28316.59

881

882

883

884

885

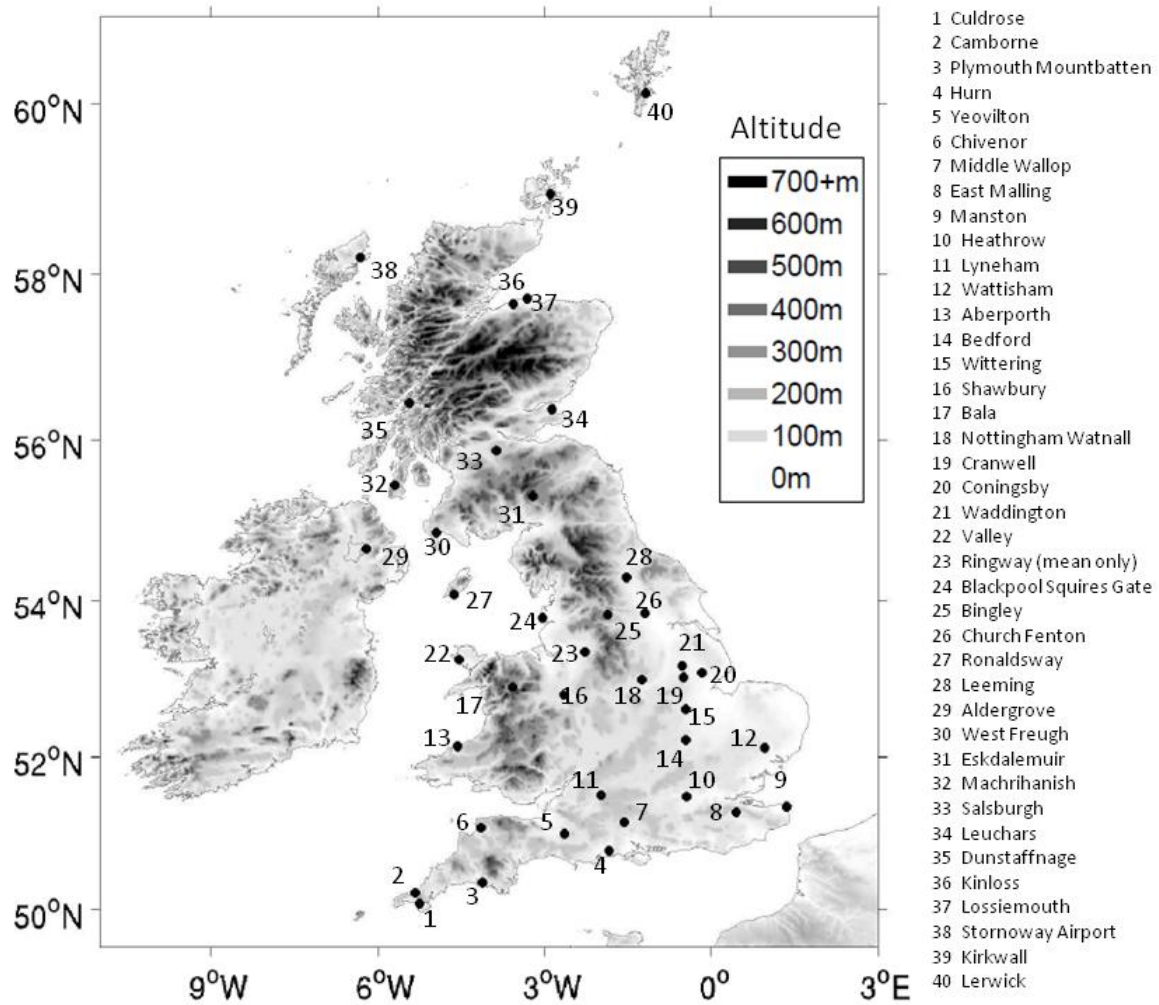
886

887 TABLE 2. Network average HM wind direction, Energy Density and daily maximum
 888 gust direction divided into compass quadrants.

Quadrant of wind direction	Percentage of Wind Direction	Percentage of Energy Density	Percentage of DMGS Wind Direction
North-east (10° - 90°)	17.9	11.1	17.5
South-east (100° - 180°)	20.2	17.8	19.6
South-west (190° - 270°)	39.8	51.8	40.2
North-west (280° - 360°)	22.2	19.3	22.7

889

890



891

892 FIG. 1. Location of observation stations in the network. Note that Ringway (23) has no
 893 DMGS data, only recording hourly mean windspeed.

894

895

896

897

898

899

900

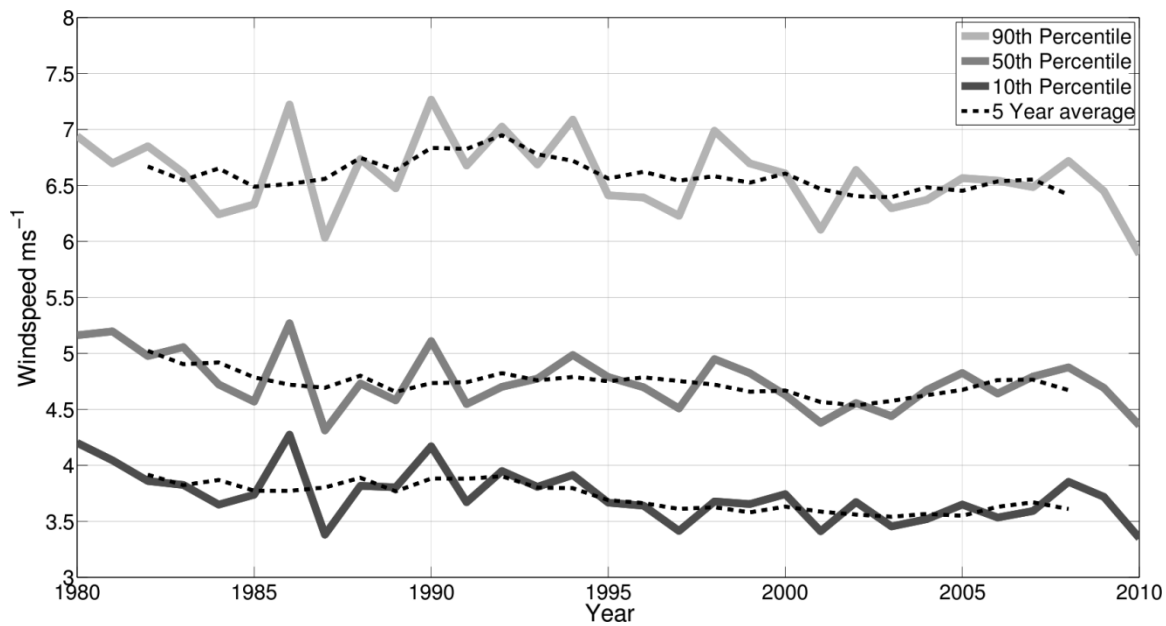
901

902

903

904

905



906
907

908 FIG. 2. 10th, 50th and 90th percentiles of annual average HM windspeeds (ms⁻¹), 1980-
909 2010, from the 40- station network.

910

911

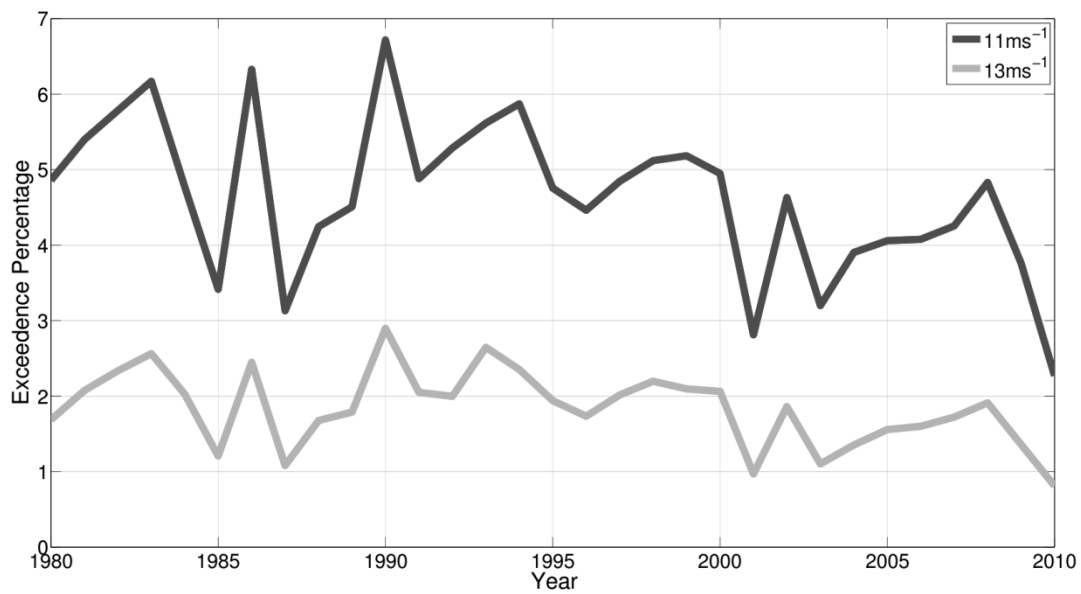
912

913

914

915

916

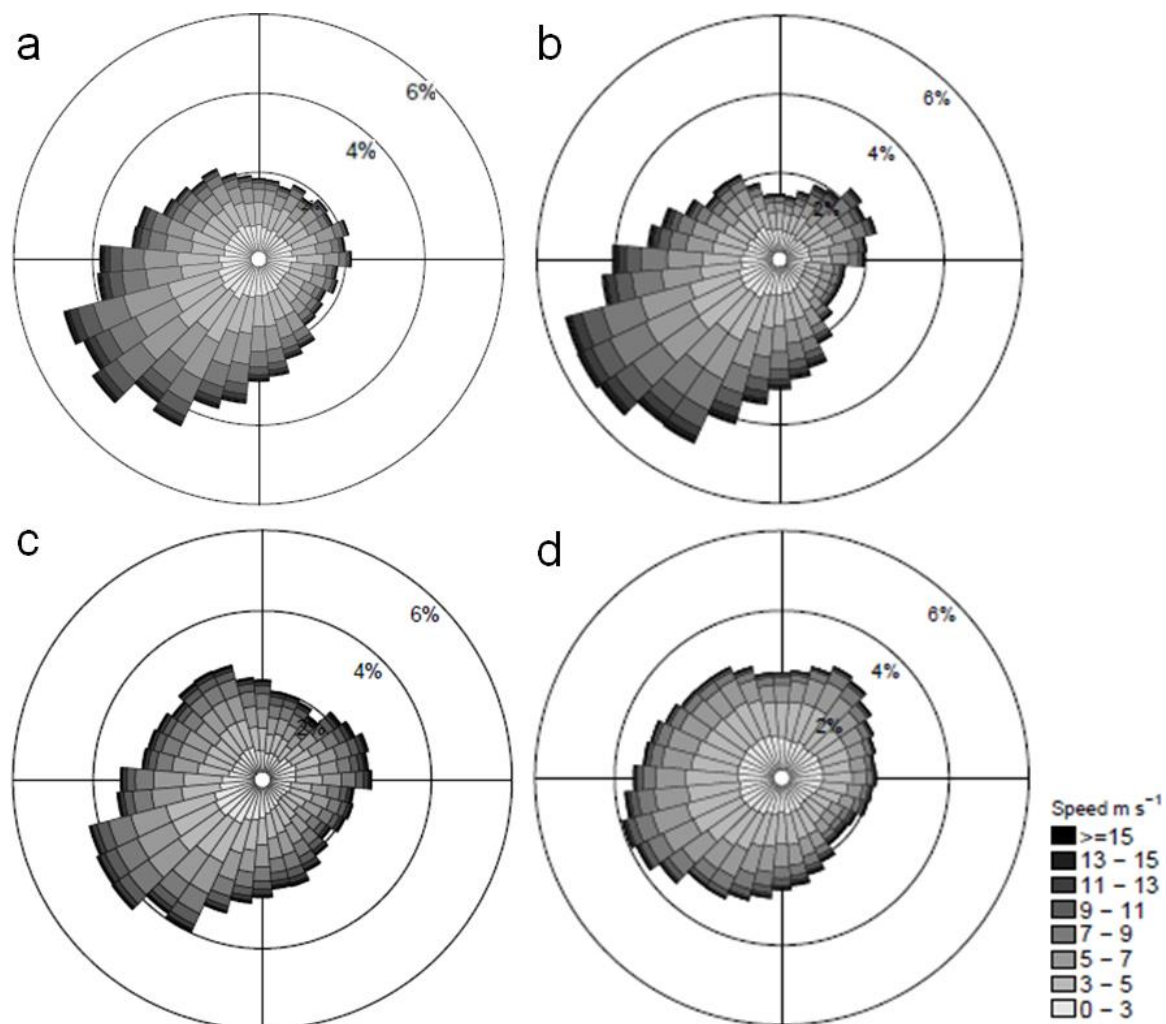


917

918 FIG. 3. Network average threshold exceedence percentages for 11 and 13ms⁻¹ HM
919 windspeeds.

920

921

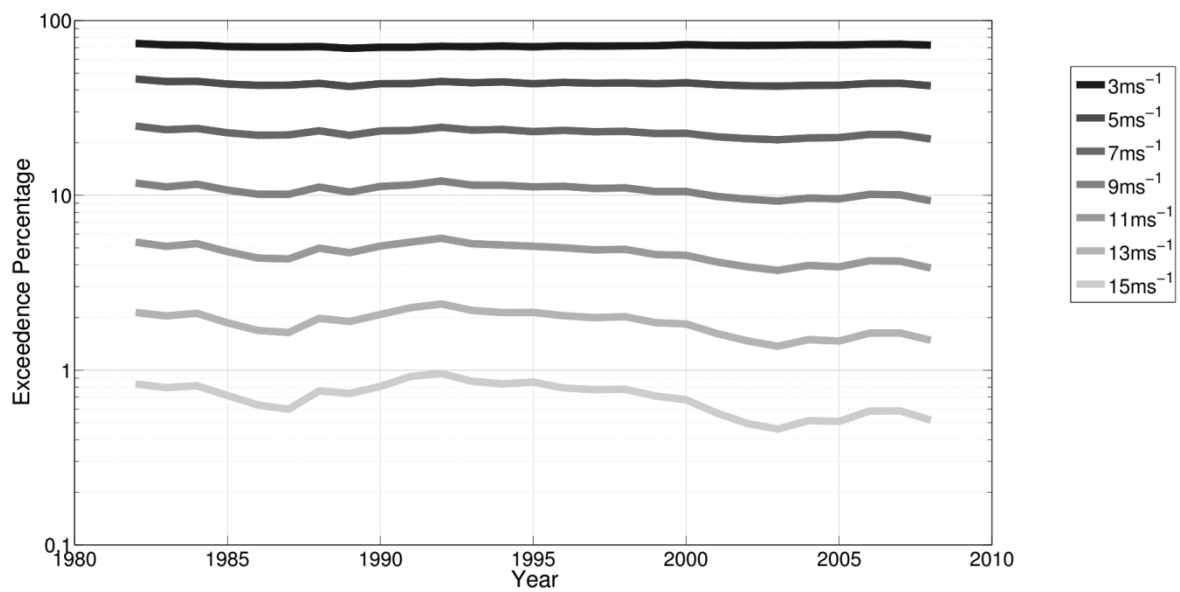


922

923 FIG. 4. Network average HM wind roses for 1980-2010 (a), 1986 (b), 1987 (c) and 2010
 924 (d).

925

926



927

928 FIG. 5. Network average 5-year running mean HM threshold exceedence percentages for
929 3, 5, 7, 9, 11, 13 and 15ms⁻¹ HM windspeeds.

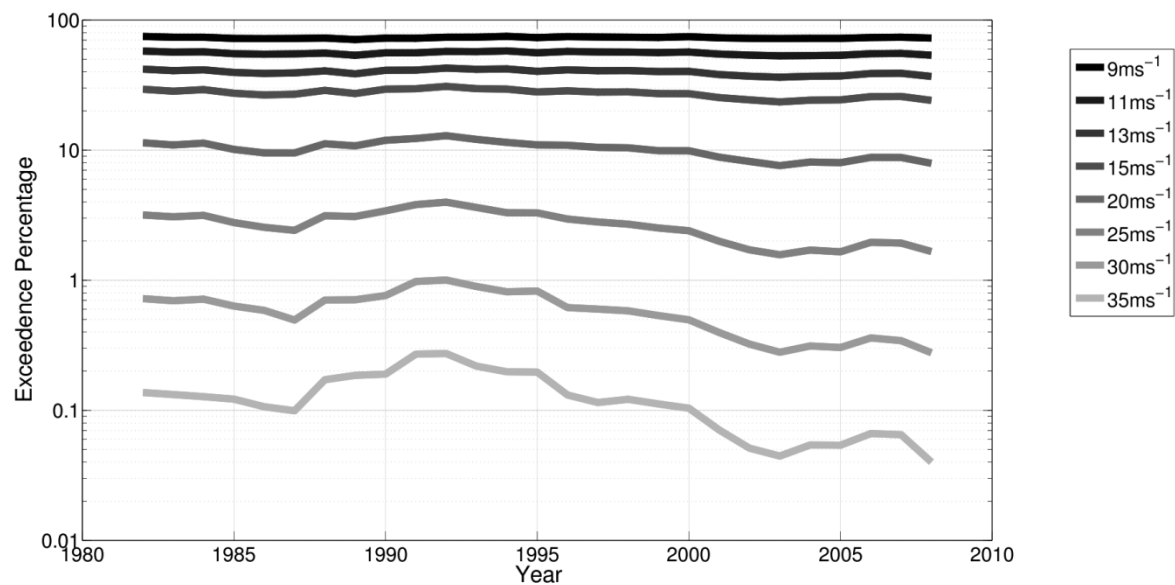
930

931

932

933

934



935

936 FIG. 6. Network average 5-year running mean threshold exceedence percentages for 9,
 937 11, 13, 15, 20, 25, 30 and 35 ms⁻¹ DMGS.

938

939

940

941

942

943

944

945

946

947

948

949

950

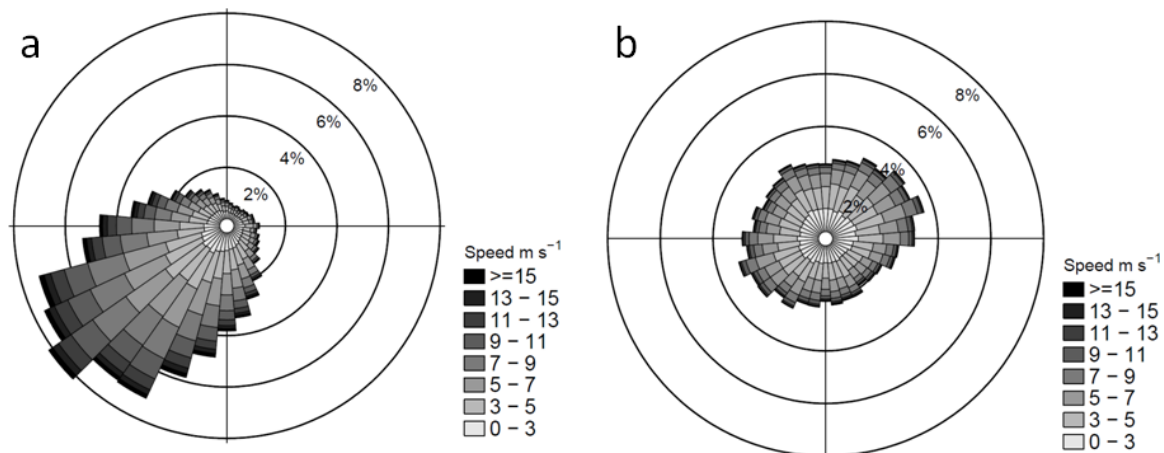
951

952

953

954

955



956

957 FIG. 7. 1980-2010 network average HM wind roses when NAO index is ≥ 2 (a) and ≤ -2
 958 (b).

959

960

961

962

963

964

965

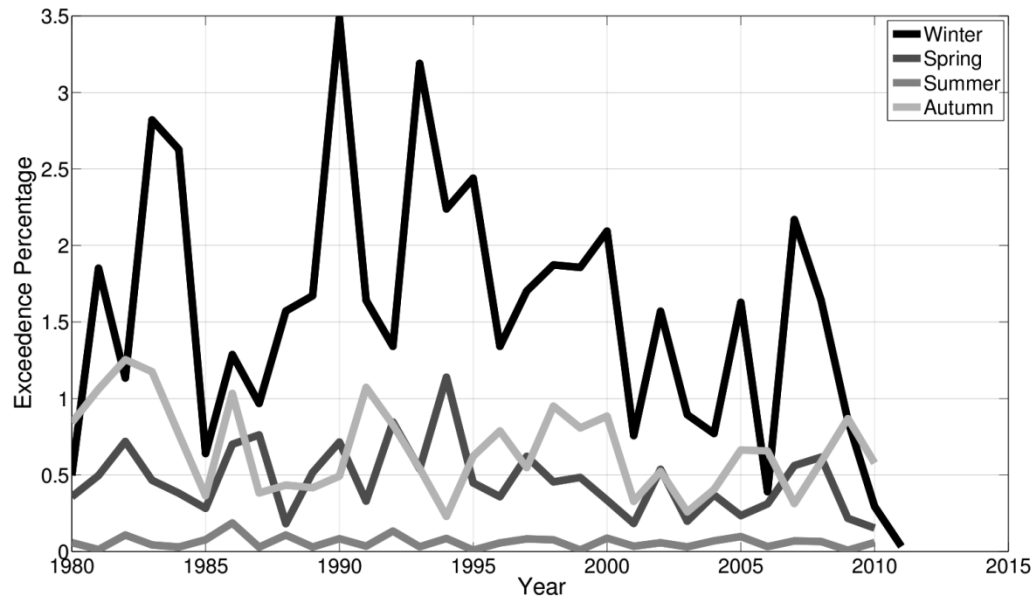
966

967

968

969

970



971

972 FIG. 8. Network average threshold exceedence percentages for 15 ms^{-1} HM windspeeds
 973 during each season, winter (DJF), spring (MAM), summer (JJA) and autumn (SON) (note
 974 that the winter of 1980 only includes Jan and Feb 1980 and the winter of 2010 only
 975 includes Dec 2010).

976

977

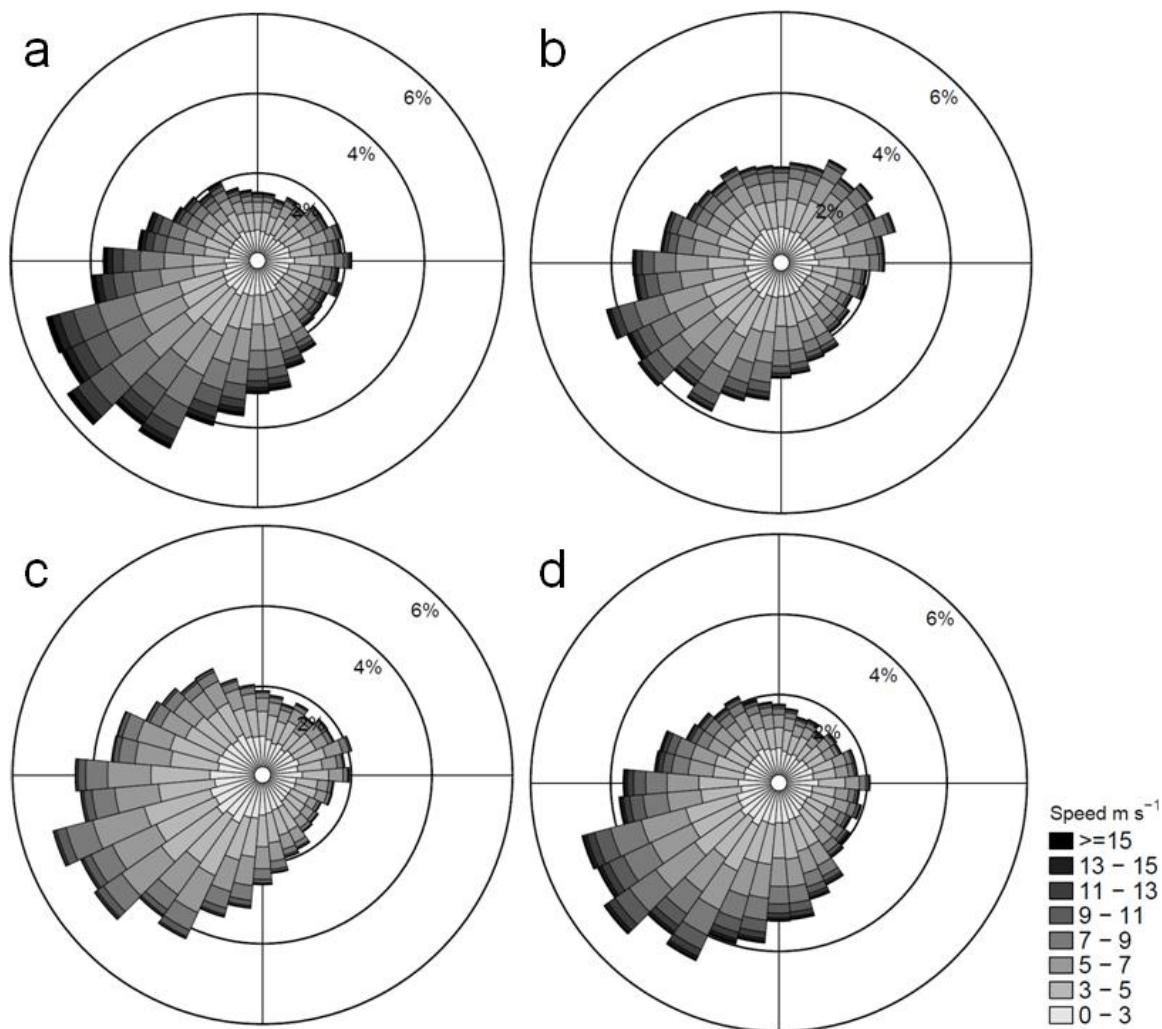
978

979

980

981

982



983

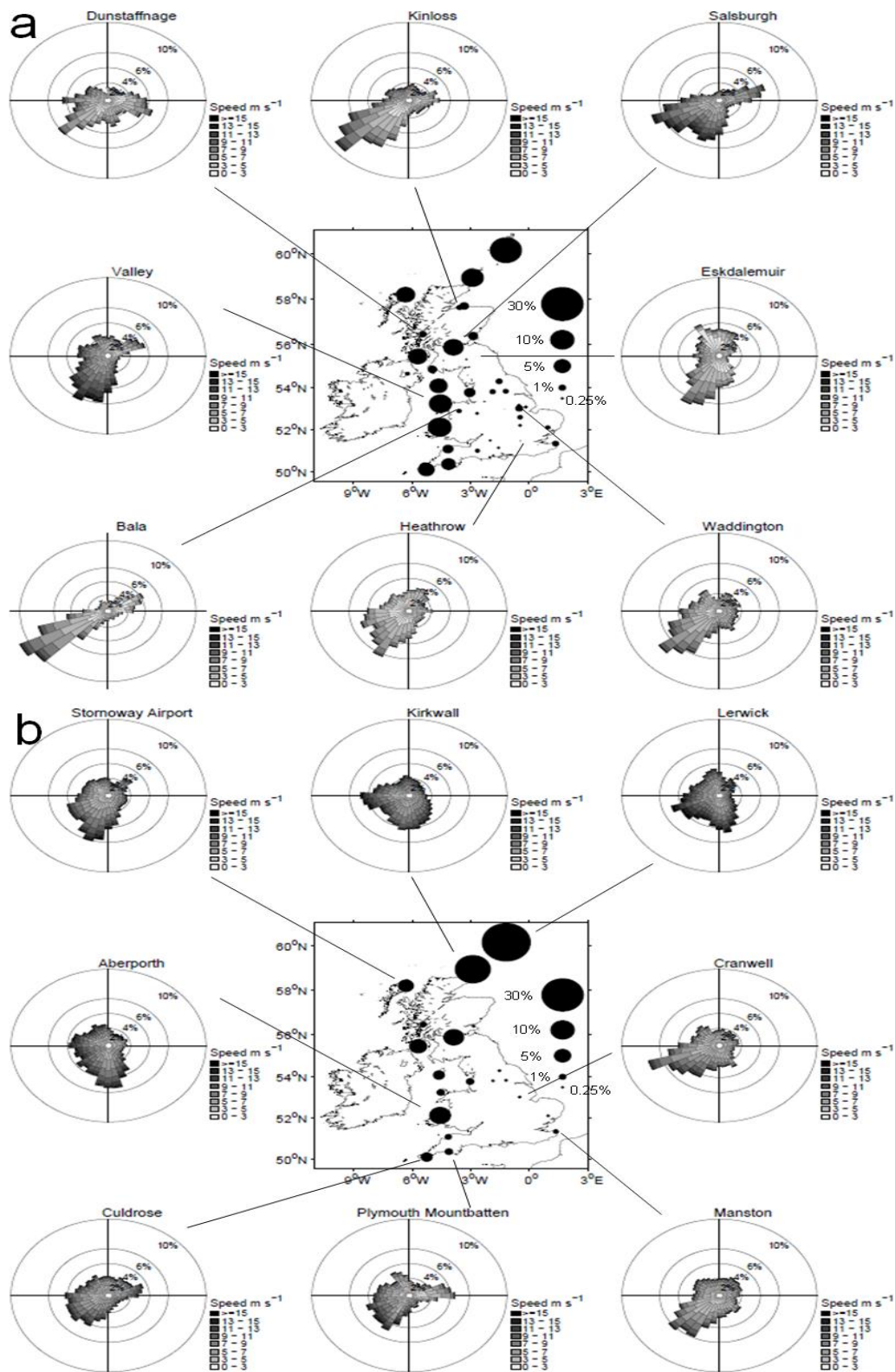
984 FIG. 9. Network average HM seasonal wind roses, 1980-2010, winter (a),
 985 summer (c) and autumn (d).

986

987

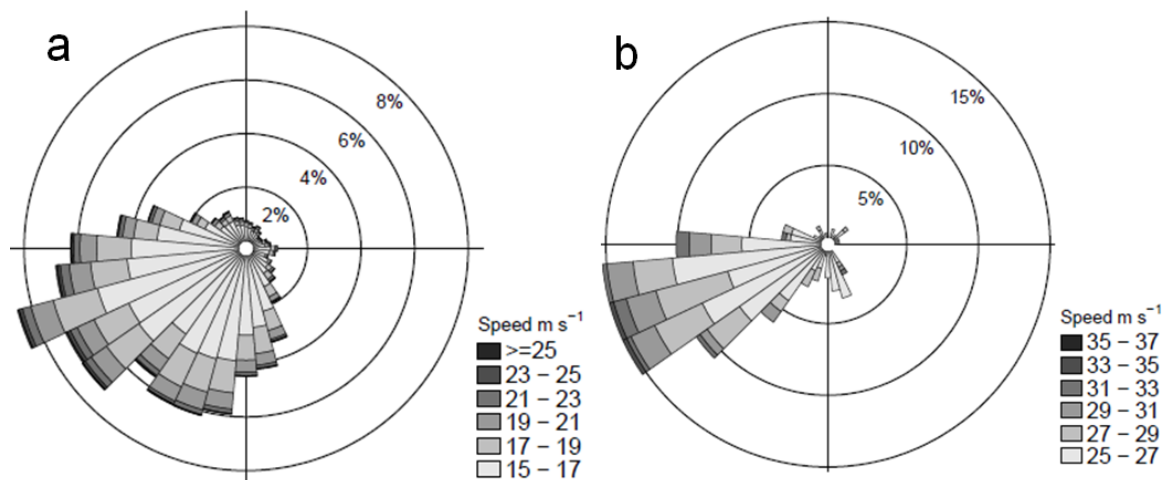
988

989



990

991 FIG. 10. Contribution (percentage) of each site to 15 ms^{-1} (a) (total counts 74154) and 25
 992 ms^{-1} (b) (total counts 323) HM windspeed threshold exceedence plus selected all-
 993 windspeed 1980-2010 individual site wind roses.



994

995 FIG. 11. 1980-2010 HM wind roses for exceedences of 15ms^{-1} (a - total counts 74154)
 996 and 25ms^{-1} (b - total counts 323) thresholds (all sites).

997

998

999

1000

1001

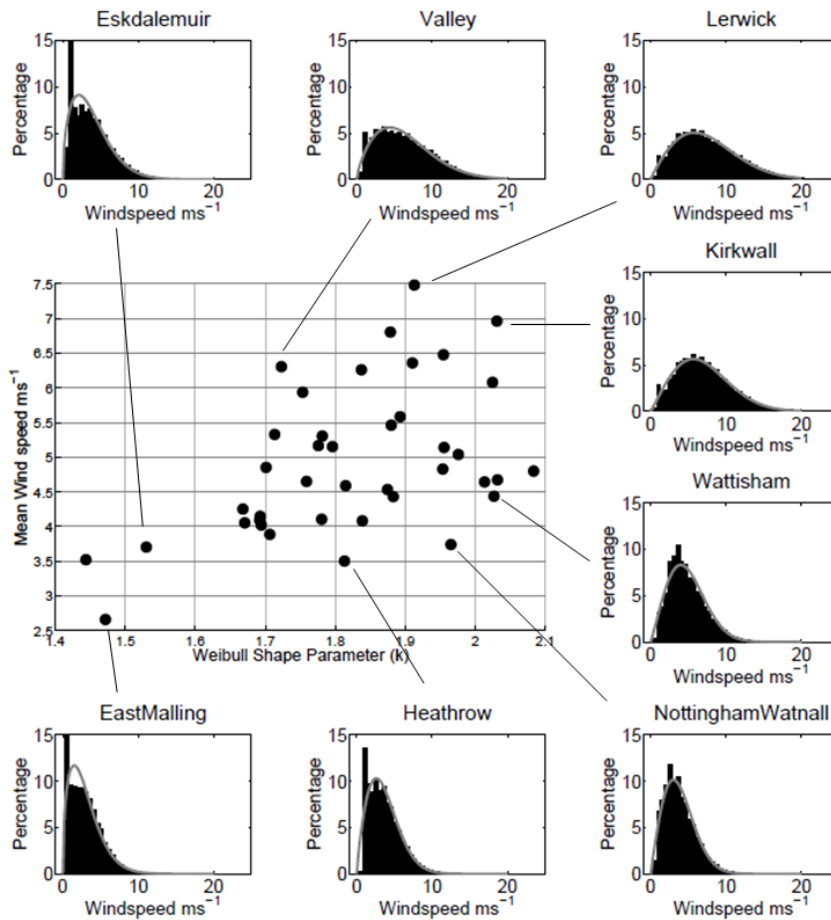
1002

1003

1004

1005

1006



1007

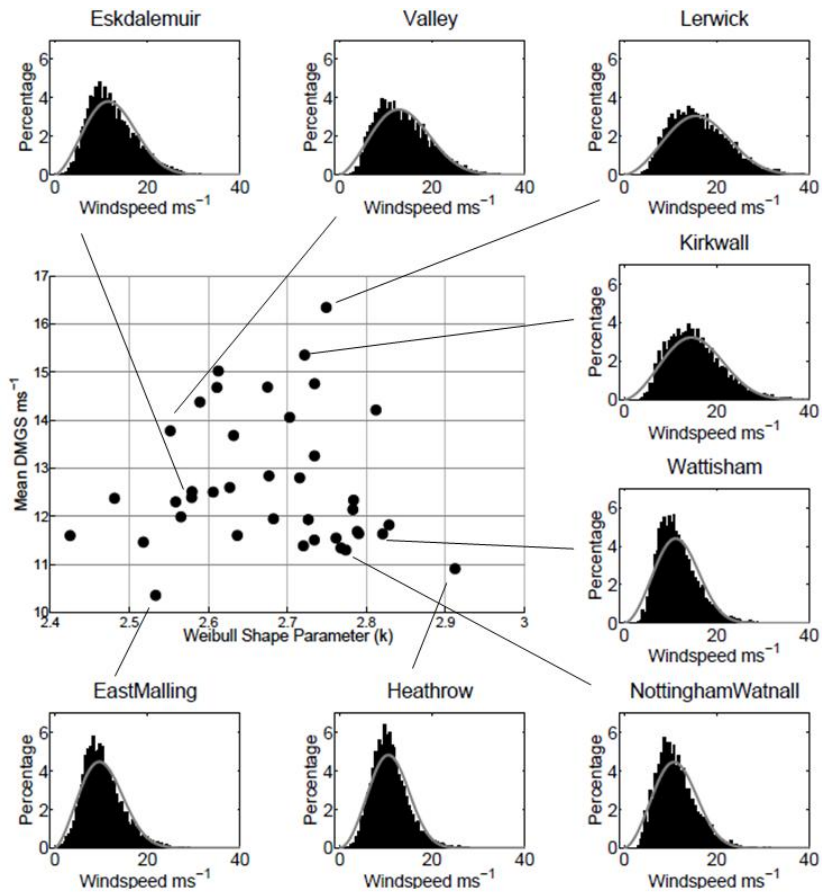
1008 FIG. 12. HM windspeeds compared with Weibull shape parameter, k , for each site plus
 1009 selected site wind distributions.

1010

1011

1012

1013



1014

1015 FIG. 13. DMGSs compared with Weibull shape parameter for each site, along with
 1016 selected site DMGS distributions.

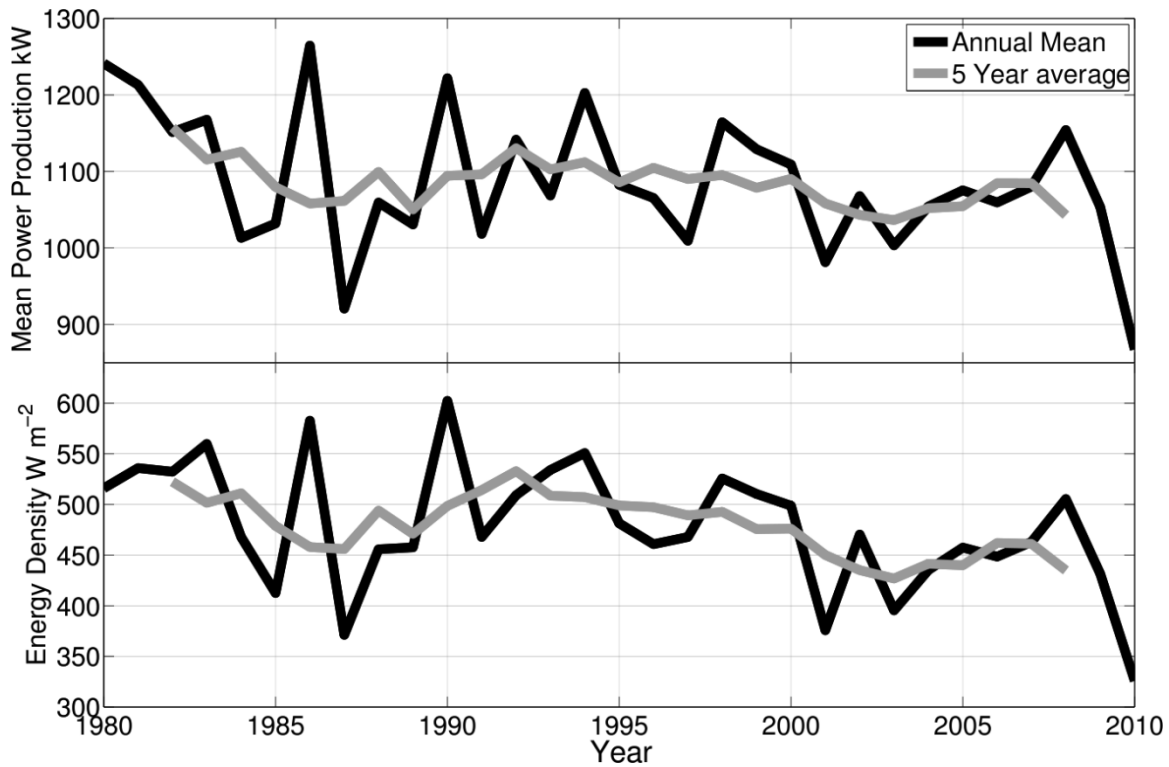
1017

1018

1019

1020

1021



1022

1023 FIG. 14. Bottom – Network average energy density ($W m^{-2}$). Top - network average
 1024 potential power output (kW) of a synthetic network of 100m hub height 3.6MW wind
 1025 turbines.

1026

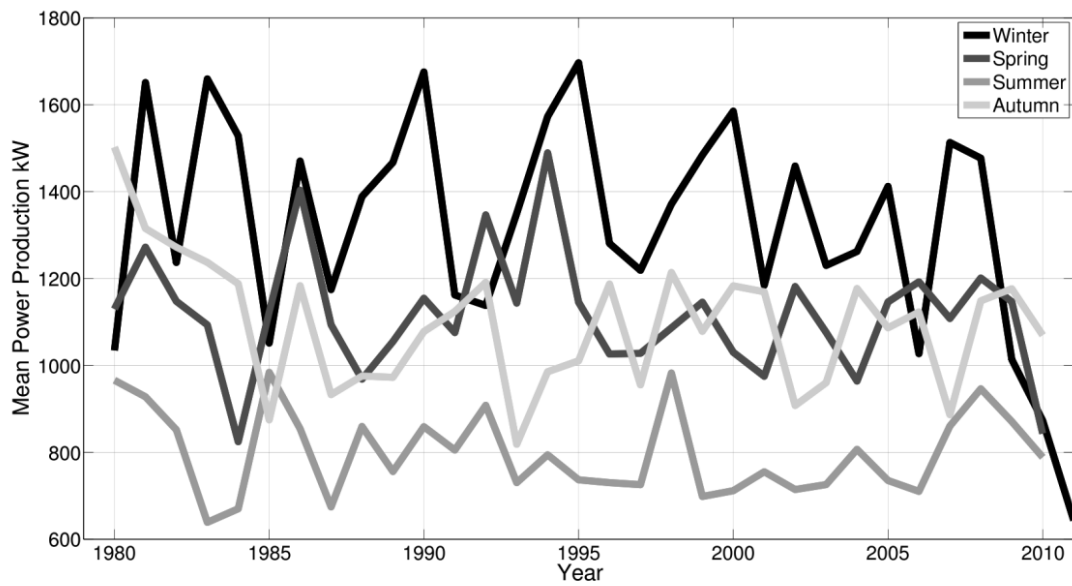
1027

1028

1029

1030

1031



1032

1033 FIG. 15. Network average seasonal mean potential power output (kW) of a synthetic
 1034 network of 100m hub height 3.6MW wind turbines (note that the winter of 1980 only
 1035 includes Jan and Feb 1980 and the winter of 2010 only includes Dec 2010).
 1036

1037